Volume 11 | Number 3 | 7 February 2024

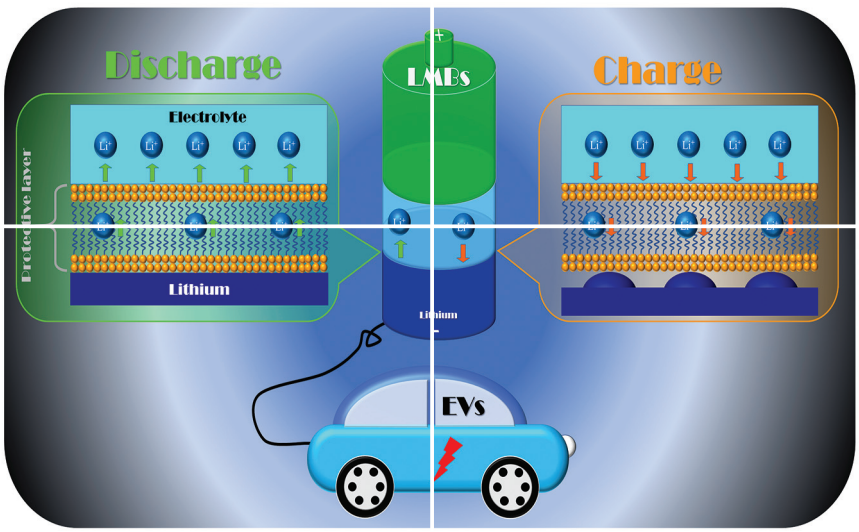

INORGANIC CHEMISTRY

FRONTIERS

CCS 中国化学会 CHINESE CHEMICAL SOCIETY
PEKING UNIVERSITY 1898
ROYAL SOCIETY OF CHEMISTRY
rsc.li/frontiers-inorganic

INORGANIC CHEMISTRY
FRONTIERS

REVIEW

View Article Online
View Journal | View Issue

Cite this: *Inorg. Chem. Front.*, 2024, **11**, 659

Interface engineering of lithium metal anodes *via* atomic and molecular layer deposition

Xiangbo Meng

Rechargeable batteries are playing an ever-increasing important role in our society. Their performance (such as cell cyclability, safety, and lifespan) is critical for their applications. Among the various factors related to cell performance, interfaces, which ubiquitously exist between an electrode and an electrolyte, have some significant functions. They mostly evolve and degrade with cell cycling. Thus, an ideal interface should be physically and electrochemically stable and able to provide a compatible environment for electrolytes and electrodes in cells. To this end, interface engineering is needed and has become an important area. It has been achieved *via* different strategies. In the last decade, atomic layer deposition (ALD) has emerged as a new strategy. It enables accurate interface modification *via* coating electrodes with desirable inorganic films at the atomic level and has created a long coating list to date. Complementarily, molecular layer deposition (MLD) extends the list to organic and organic–inorganic hybrid coatings. More amazingly, their combinations could further make the list uncountable. Owing to numerous efforts using ALD and MLD for advancing lithium-ion batteries (LIBs), there has recently been an ever-growing interest in lithium metal batteries (LMBs). In this review, we focus on summarizing the studies addressing the most forbidding issues of lithium metal anodes in LMBs using ALD and MLD. The inherent merits of ALD and MLD have made them two irreplaceable tools for opening up new technical avenues to commercialize LMBs.

Received 30th October 2023,
Accepted 2nd January 2024

DOI: 10.1039/d3qi02241b

rsc.li/frontiers-inorganic

1. Introduction

Fossil fuels (coal, gas, and oil) have been serving as our main energy supplies in the past century, accounting for over 80% of the total energy consumed annually. Such continuous huge consumption is leading to quick depletion while causing many environmental issues and changing our ecosystems. To tackle these challenges for achieving a long-term sustainable society, electrification is promising and can facilitate the wide implementation of renewable energies such as solar and wind power. To this end, portable electrical energy storage (EES) systems are critical, which store electricity harvested from renewable energy sources and supply it to energy-consumption sectors, *e.g.*, portable electronics, electric vehicles (EVs), and smart grids. In this respect, lithium-ion batteries (LIBs) are to date the most successful EES devices playing a dominant role in portable electronics. Additionally, transportation electrification is significant, as transportation is consuming nearly one third of the total energy.[1] Currently, LIBs are penetrating the EV market, while governments worldwide are setting various programs to spur EV sales. In this context, better batteries are urgently needed, as state-of-the-art LIBs are still insufficient in multiple aspects, including energy density, cost, safety, and lifetime.[2–4] A desirable battery technology for EVs needs to satisfy an energy density of ≥300 W h kg^{-1}, low cost (≤$125 kW per h), long lifespan (≥15 calendar years), and reliable safety free of fire and explosion.[5–7]

To radically boost the market share of EVs, lithium metal batteries (LMBs) have been proposed and undergoing intensive investigation, featuring the replacement of graphite anodes in LIBs with lithium metal (Li) anodes. This change promises a much higher energy density of LMBs, as the Li metal has the lowest negative electrochemical potential (−3.04 V *versus* the standard hydrogen electrode) and the highest theoretical capacity of 3860 mA h g^{-1} at room temperature, more than 10 times higher than that of the graphite anodes (372 mA h g^{-1}) in LIBs.[8–12] Consequently, the Li metal has been regarded as an ultimate anode material and can be used to couple with nearly any cathode to constitute an LMB cell. The cathodes can be any existing cathodes used in LIBs such as $LiCoO_2$ (LCO), $LiMn_2O_4$ (LMO), $LiFePO_4$ (LFP), $LiNi_xMn_yCo_zO_2$ (NMCs, $x + y + z = 1$), and $LiNi_xCo_yAl_zO_2$ (NCAs, $x + y + z = 1$). They also can be any emerging cathodes such as sulfur (S) and oxygen (O_2). Thus, there are a variety of LMBs under development.

Although LMBs are very promising, their commercialization is a challenge. Their limitations are closely related to electrodes (Li metal anodes and cathodes), electrolytes, and interfaces between them. Traditionally, organic liquid electrolytes

Department of Mechanical Engineering, University of Arkansas, Fayetteville, AR 72701, USA. E-mail: xbmeng@uark.edu

(oLEs) are widely used in LIBs, while solid-state electrolytes (SEs) are undergoing extensive investigation. SEs can be polymeric (*i.e.*, pSEs), inorganic (iSEs), or composite (cSEs). No matter what electrolyte is applied in an LMB system, the interface between the electrode (either an Li metal anode or a cathode) and the electrolyte plays a prominent role, which has some significant impacts on the resulting cell's performance. Owing to the highly negative electrochemical potential of Li^+/Li, any electrolyte can be readily reduced at the Li surface with the production of a layer of solid electrolyte interphase (SEI). However, electrolytes are prone to oxidation at cathodes at high potentials to form a layer of cathode electrolyte interphase (CEI). Both SEI and CEI are mosaic in composition and heterogenous in ionic conductivity. As a result, Li^+ ions may deposit preferentially and grow into dendritic structures on the Li anode side during an Li plating process. The resulting Li dendrites are in core–shell structures, *i.e.*, having an Li metal core and an SEI shell. They may grow into the cathode side and thereby get the cell shorted. Thus, Li dendrites pose serious safety issues.

In summary, the Li metal suffers from two main issues: high reactivity to electrolytes with the production of SEI and dendritic growth during plating. Particularly, the Li dendritic growth and SEI formation are interconnected and self-accelerated. This makes the use of Li metal as a practical anode very difficult, hampering the commercialization of LMBs. To address these two issues of Li metal anodes for commercializing LMBs, there have been an increasing number of efforts reported in the literature. Among the various efforts, surface coating has been an important strategy to practice interface engineering of Li anodes. It is important that a coating should be applied on Li anodes at a temperature lower than the melting point of the Li metal of ~180 °C. It should be uniform, conformal, and tunable for achieving desirable properties. Traditional deposition techniques are unsatisfactory for this. Chemical vapor deposition (CVD),[13] for instance, requires high temperatures (*e.g.*, 600 °C or higher), while physical vapor deposition (PVD), *e.g.*, sputtering and vaporization,[14] suffers from its limited material choices and its line-of-sight deposition nature. Furthermore, they both are unable to control the coating thickness accurately. In this context, atomic and molecular layer deposition (ALD and MLD) have emerged as two unique vapor deposition tools, showing excellent capabilities to provide novel solutions, ascribed to their distinctive merits including low process temperature (≤150 °C), extremely uniform and conformal coating, and unlimited material choices.[15,16] Since their first application in LIBs at the very beginning of the 2000s, they have been well recognized as two important techniques for interface engineering of rechargeable batteries.[17–19] In this work, we focus on summarizing the recent progresses of ALD and MLD for interface engineering of Li metal anodes in LMBs and showcase the most encouraging studies. We expect that this effort would shed some light on the applications of ALD and MLD for interface engineering of Li metal anodes and stimulate many more efforts using them to develop new technical solutions for LMBs.

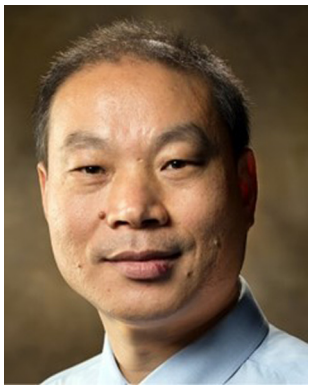

Xiangbo Meng

Xiangbo Meng is currently an Associate Professor in the Department of Mechanical Engineering at the University of Arkansas (Fayetteville, AR). He received one PhD degree in Mechanical & Materials Engineering (2011) and another in Chemical & Biochemical Engineering (2008), both from the University of Western Ontario (ON, Canada). Prior to joining the University of Arkansas in 2016, he was a Research Fellow (2012–2016) in Energy Systems Division at Argonne National Laboratory (Lemont, IL) and a Research Associate (2011–2012) in the Chemistry Department at Brookhaven National Laboratory (Upton, NY). He was the recipient of a Canada NSERC Postdoctoral Fellowship (2011–2013), the AVS Student Award in ALD (2011), and the 2nd Prize of OCE Competition (2008). He was also the nominee of the Canadian CGS/UMI Distinguished Dissertation Award (2009) and Moore Inventor Fellows (2017). His interests lie in smartly designing novel nanostructured materials for a wide range of applications such as energy, catalysis, semiconductors, surface engineering, and biomedicine. Currently, Dr Meng's research focuses on developing new chemical processes for growing new inorganic, organic, and hybrid nanomaterials in a precisely controllable mode using both atomic and molecular layer deposition (ALD and MLD), and on developing high-performance advanced battery systems, including lithium-ion batteries, lithium–sulfur batteries, sodium-ion batteries, solid-state batteries, and microbatteries.

2. Briefing on ALD and MLD

ALD and MLD are two sister vapor-phase thin film techniques, sharing analogous growth mechanisms that make them possible to accurately control material growth. ALD is exclusively used for growing inorganic materials at the atomic level, while MLD is used specifically for growing organic or organic–inorganic hybrid materials at the molecular level.[20] They both commonly rely on alternative self-limiting surface reactions to achieve material growth in a layer-by-layer mode. As illustrated in Fig. 1a, the growth mechanism of ALD is exemplified by the model process of Al_2O_3 using trimethylaluminum (TMA, $Al(CH_3)_3$) and H_2O as precursors. It proceeds with two half-reactions alternatively on the substrate surface, as described in equations of (1A) and (1B) as follows:[21]

$$|\text{–OH} + \text{Al}(\text{CH}_3)_3(\text{g}) \rightarrow |\text{–O–Al}(\text{CH}_3)_2 + \text{CH}_4(\text{g}) \quad (1\text{A})$$

$$|\text{-O–Al}(\text{CH}_3)_2 + 2\text{H}_2\text{O}(\text{g}) \rightarrow |\text{–OAl}(\text{OH})_2 + 2\text{CH}_4(\text{g}) \quad (1\text{B})$$

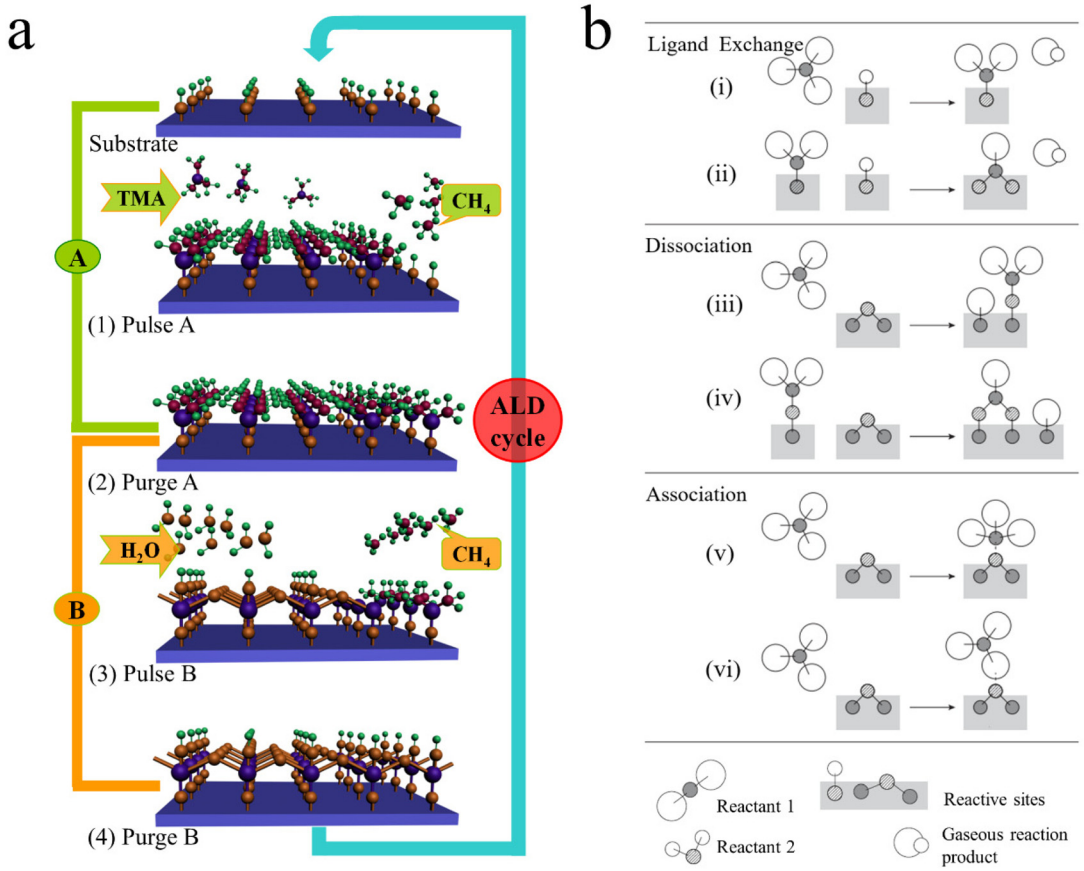

Fig. 1 Schematic illustrations of (a) the ALD process, which is exemplified by that ALD Al_2O_3 using TMA and water as precursors[17] and (b) the chemisorption mechanisms possible in ALD.[22] Reprinted with permission from ref. 17. Copyright (2012) John Wiley & Sons. Reprinted with permission from ref. 22. Copyright (2003) John Wiley & Sons.

where "|" indicates substrate surfaces while "(g)" signifies gas phases. The surface chemistry of the ALD Al_2O_3 is mainly based on ligand exchanges between –OH and $–CH_3$ to arrange atoms accurately in a layer-by-layer fashion. In addition to ligand exchange, there are two other chemisorption mechanisms for the surface chemistry of ALD processes: dissociation and association (as illustrated in Fig. 1b).[22,23] The self-limiting or self-terminating nature of the surface reactions is typically caused by either of the two factors: steric hindrance of ligands and limited number of bonding sites.[22] This has further determined the growth accuracy of ALD and its other unique characteristics. The four steps (from 1 to 4 in Fig. 1a, *i.e.*, pulse **A**/purge **A**/pulse **B**/purge **B**) constitute one ALD cycle and they can repeat to build up films for a desired thickness. With suitable precursors, ALD theoretically can grow any inorganics and has to date produced a large variety of materials[24,25] including elements, oxides, sulfides, nitrides, and fluorides.

Analogous to ALD mechanistically, MLD can accurately grow pure and hybrid polymers with an accuracy at the molecular level. The molecular-level accuracy is determined by the long chains of MLD organic precursors. In case of growing pure polymers (Fig. 2a), the molecules of the precursor **A** first react with the reactive sites of a substrate *via* a corresponding linking chemistry to add a molecular layer with new reactive sites on the substrate surface.[26] Following a thorough purge **A**, the molecules of the precursor **B** react with the new reactive sites, thereby producing another molecular layer and recovering the surface back to the initial reactive groups. Another full purge **B** is performed to finish one MLD cycle. Through repeating the afore-discussed four steps, one can achieve the desired film thickness *via* MLD. Using adipoyl chloride (AC) and 1,6-hexanediamine (HD) as precursors,[27,28] for example, an MLD process has been developed for growing nylon films linearly and the surface chemistry is described as follows:

$$|-NH_2 + ClCO(CH_2)_4COCl(g) \rightarrow |-NHCO(CH_2)_4COCl + HCl(g) \quad (2A)$$

$$|-NHCO(CH_2)_4COCl + H_2N(CH_2)_6NH_2(g) \rightarrow |-NHCO(CH_2)_4CO-NH(CH_2)_6NH_2 + HCl(g). \quad (2B)$$

The AC-HD MLD process could realize a growth per cycle (GPC) of 19 Å per cycle at 62 °C.[28] It is apparent that the molecular layers of $–CO(CH_2)_4CO–$ and $–NH(CH_2)_6NH–$ during the MLD-nylon are much larger than the atomic layers of –Al– and –O– in the ALD-Al_2O_3. This underlies the higher GPC of the

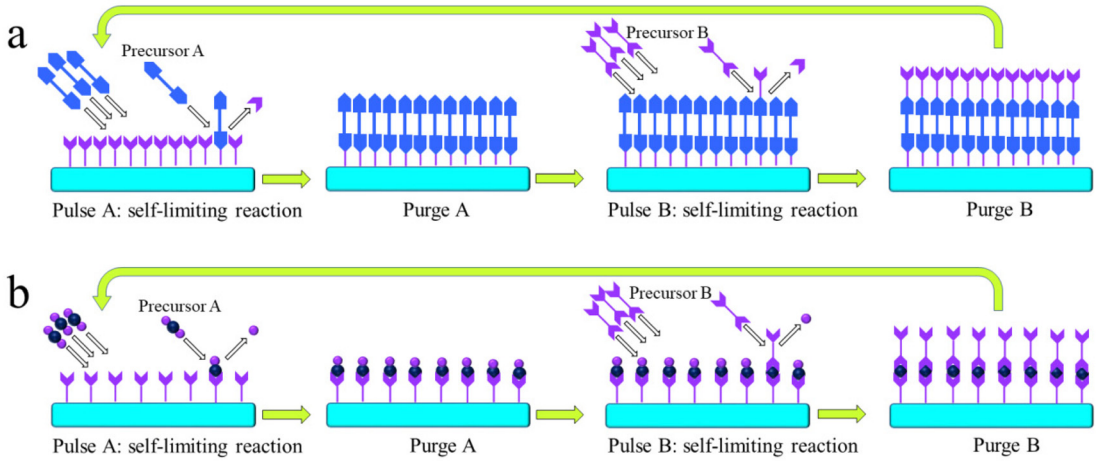

Fig. 2 Schematic illustrations of the MLD processes for growing (a) pure polymers and (b) organic–inorganic hybrid films.

MLD nylon process of AC-HD. Additionally, many more pure polymeric materials *via* MLD have been recently reported,[20] and they are polyazomethines,[29–32] polyureas,[33–37] polyamides,[27,28,38,39] poly(3,4-ethylenedioxythiophene),[40,41] polyimide-polyamides,[42] polythioureas,[43] polyethylene terephthalate,[44] and the others.[45,46]

In addition to pure polymeric films, MLD also enables organic–inorganic hybrids by adopting an ALD precursor and an MLD precursor (Fig. 2b), such as metal alkoxide materials (*i.e.*, metalcones), in which diols can be used to couple with a metal precursor. For instance, a metal-based hybrid polymer can be synthesized using TMA and ethylene glycol (EG, $HOCH_2CH_2OH$, and a homobifunctional diol precursor). The resulting hybrid (*i.e.*, AlEG, $Al(OCH_2CH_2O)_2$) is an aluminum alkoxide (*i.e.*, alucone) and its MLD surface chemistry can be described using the following reactions:[47]

$$|\text{–OH} + \text{Al}(\text{CH}_3)_3(\text{g}) \rightarrow |\text{–O–Al}(\text{CH}_3)_2 + \text{CH}_4(\text{g}) \quad (3\text{A})$$

$$\begin{aligned} &|-\text{O}-\text{Al}(\text{CH}_3)_2 + 2\text{HOCH}_2\text{CH}_2\text{OH}(\text{g}) \\ &\quad\rightarrow |-\text{OAl}(\text{OCH}_2\text{CH}_2\text{OH})_2 + 2\text{CH}_4(\text{g}) \end{aligned} \quad (3\text{B})$$

Apparently, the molecular fragment of $–OCH_2CH_2O–$ attached in the MLD alucone is far much larger than the atomic part of –O– in ALD Al_2O_3. This well explains that the resulting alucone has grown much faster than ALD Al_2O_3, accounting for 4 Å per cycle at 85 °C for the MLD alkoxide[47] *versus* 1.3 Å per cycle for ALD Al_2O_3 at 80 °C.[21] Through smartly selecting precursors for their functional groups and backbones, MLD enables developing different metalcones or hybrid materials with desired properties. Substituting EG with the aromatic hydroquinone (HQ, HOC_6H_4OH), for example, another alucone has been deposited, which has its surface chemistry as follows:[48]

$$|\text{–OH} + \text{Al}(\text{CH}_3)_3\ (\text{g}) \rightarrow |\text{–O–Al}(\text{CH}_3)_2 + \text{CH}_4\ (\text{g}) \quad (4\text{A})$$

$$\begin{aligned} &|\text{–O–Al}(\text{CH}_3)_2 + 2\text{HOC}_6\text{H}_4\text{OH}\ (\text{g}) \\ &\quad\rightarrow |\text{–OAl}(\text{OC}_6\text{H}_4\text{OH})_2 + 2\text{CH}_4\ (\text{g}). \end{aligned} \quad (4\text{B})$$

This TMA-HQ MLD process exhibits a GPC of 4.1 Å per cycle at 150 °C.[48] Alucones with different backbones are expected to exhibit different properties. The aromatic backbone of HQ is expected to provide structural stability and contribute largely to the electrical properties of the resulting polymer films. To date, many more metalcones including alucones,[47–76] zincones,[57,77–84] titanicones,[57,77–86] vanadicones,[87] zircones,[88,89] hafnicones,[90] mangancones,[62] metal quinolones,[91,92] and some other hybrid materials[93–108] have been reported.

The growth rate of both ALD and MLD is described by GPC. GPC is related to three parameters: precursor, processing temperature, and substrate.[22,23] Relying on the surface chemisorption to proceed with surface reactions while requiring no decomposition of precursors, consequently,[23] the temperatures of ALD and MLD processes are generally low, typically no more than 300 °C. Adopting precursor pairs with high reactivity, the resulting ALD and MLD processes can be achieved at temperatures less than 100 °C and even room temperature (25 °C).[109–111] The low processing temperature of ALD and MLD processes makes it possible to utilize some biological and polymeric templates unstable at high temperatures for some emerging applications.[112] Ascribed to their unique layer-by-layer growth mechanism with accurate controllability, ALD and MLD can realize extremely uniform deposition over large-scale two-dimensional (2D) planar substrates with a minimum roughness. For example, atomic force microscopy (AFM) has revealed a surface roughness of 1–3 Å for ALD Al_2O_3 deposition in the range of 200–560 Å.[113–115] A typical MLD film roughness is in the range of 2–6 Å.[20] The ALD/MLD-induced uniform films can also be realized on substrates with a large variety of morphologies, leading to conformal coatings. Thus, ALD and MLD feature their unparalleled capacities mainly in the following aspects: low processing temperature, precise growth accu-

racy, extremely uniform and conformal coverage, and a long list of inorganic, organic, and hybrid materials as thin films.

Thanks to the unmatched merits as thin film techniques, ALD and MLD have been gaining an ever-increasing attention for modifying interfaces of various advanced batteries in the past decade. The first report of the ALD practices in batteries was about an ALD TiN process in 2007, which was used to coat an $Li_4Ti_5O_{12}$ (LTO) anode powder to improve the resulting LTO anode's conductivity.[116] Later in 2010, two significant studies by Jung *et al.* for the first time reported that sub-nano ALD coatings (<1 nm) could be applied not only on electrode powders but also on prefabricated electrodes.[117,118] Since then, a new area has been formally unveiled for ALD and MLD as two novel tools to practice interface engineering of rechargeable batteries. Thus far, the choices of surface coatings *via* ALD have been greatly enriched, ranging from nitrides[116] and oxides[117–121] to fluorides,[122,123] sulfides,[124] phosphates,[125] and oxynitrides.[126] Besides LIBs, ALD has been attracting increasing attention for developing new batteries including Li–S,[127,128] Li–O_2,[129] Na-based,[130] K-based,[131] Zn-based,[132] and Al-based batteries.[133] In the case of MLD, Leobl *et al.*[58] was credited to the first attempt of MLD with an alucone coating for modifying LIBs in 2013. Subsequently, numerous studies of MLD polymeric coatings have been reported for modifying Si anodes,[71] Li metal anodes,[134] Na metal anodes,[135] and cathodes of Na-ion batteries.[136]

Striving for addressing the two challenging issues (*i.e.*, continuous formation of SEI and dendritic growth), many strategies and techniques have been applied. Among them, ALD and MLD have been recently demonstrated as two very promising techniques for novel coatings to tackle the issues of Li anodes. These efforts of ALD and MLD in interface engineering of LMBs are exhibited in three functionalization aspects: (1) surface coating of Li anodes, (2) tuning lithiophilicity of current collectors to facilitate Li deposition, and (3) constituting three-dimensional (3D) current collectors for hosting Li deposition, which will be introduced in detail in the following sections of this work.

3. Surface coating of Li anodes

Surface coating is a facile and effective strategy to practice interface engineering of Li metal anodes. To protect the underlying Li metal, a desirable coating is expected to exhibit the following merits: (1) chemically stable in a highly reducing environment, (2) excellent ionic conductivity to facilitate Li stripping and plating, (3) exceptional electrical insulator to ensure no plating above the interface, (4) sufficient mechanical strength to sustain its integrity and inhibit lithium dendritic growth, (5) uniform film composition and properties, (6) high film quality free of defects, and (7) good adhesion on Li metal. ALD and MLD are distinguished by their unparalleled capabilities, *i.e.*, low process temperatures (≤150 °C), uniform and conformal coverage, accurate control of coating thickness at the atomic and molecular level, and strong viability for numerous films ranging from inorganic to organic and hybrid materials.[15,17,20,23,24] To date, a variety of inorganic and organic coatings *via* ALD and MLD have been investigated. They still could not satisfy all these afore-mentioned desirable merits but showed promising protection effects on Li anodes.

Due to the high reactivity of Li metal to air and moisture, it is important to avoid exposures during handling and transferring Li metal samples before and after surface coating *via* ALD or MLD. To do so, the ALD or MLD system is integrated with a glove box, as reported in the literature.[137,138] Owing to the low melting point of Li metal (~180 °C), in addition, the ALD or MLD can be performed at a temperature lower than 180 °C. In this respect, a large variety of ALD or MLD processes were possible at a temperature ≤150 °C, as reported in the literature.[137–140]

3.1. Inorganic surface coatings *via* ALD

The first practice of ALD on Li anodes was started from Al_2O_3,[139,140] followed by ZrO_2,[141] TiO_2,[142] LiF,[143] Li_3PO_4,[144] and Li_xAl_yS (LAS).[124] These ALD coatings are mainly thin, less than 15 nm. These studies verified that surface coating *via* ALD is effective in improving the cyclability of Li||Li symmetric cells, Li||Cu asymmetric cells, and Li||cathode LMB full cells. They served as protective films, which protected Li metal from oxidation and inhibited Li plating from dendritic growth. Among them, except for LAS being air-sensitive, the others could protect the Li metal from oxidation in air for varying durations, depending on the coatings' thicknesses.[139,141,142,144] Thicker coatings could protect the Li metal longer, up to several tens of hours. In comparison, the bare Li metal turned into black in air in a very short time, 1–5 min, due to its reaction with oxygen and moisture in the air. Additionally, it has also been confirmed that a 190 nm-thick ZrO_2 coating could improve the thermal tolerance and shape the integrity of the Li metal.[141] All these surface coatings obtained *via* ALD have been examined to verify if they could suppress the formation of Li dendrites in a certain number of Li-stripping/plating cycles. During Li-stripping/plating processes, these thin ALD coatings might gradually diffuse into Li and got loss completely. For example, Al_2O_3 and TiO_2 have been suggested to transform into $Li_xAl_2O_3$ [139] and $Li_2Ti_2O_4$.[142] Thus, there might be a gradual evolution process for these coating layers and this process might have limited their lifetime.

Besides the oxide coatings, three Li-containing coatings, namely, LiF,[143] Li_3PO_4,[144] and LAS[124] were studied to date. LiF is the main component of an SEI layer in LIBs. It is electrochemically stable from 0 to 6.4 V,[145] electronically insulating, and has a relatively high shear modulus of 55 GPa.[146] The shear modulus of a coating layer is critical in suppressing Li dendrites. The Li metal has a shear modulus of 4.25 GPa.[147] It was suggested by Monroe and Newman that the shear modulus should be at least twice (>8.5 GPa) that of the Li metal in order to prevent dendrite nucleation.[148] Chen *et al.* demonstrated with nanoindentation that the crystalline LiF film obtained *via* ALD has a sheer modulus of 58 GPa, 6–7 times higher than the value required to suppress Li dendrites.[143] They also revealed

that the ALD LiF coating has an ionic conductivity of 10^{-14} S cm^{-1} at room temperature. Furthermore, they demonstrated that an 8 nm-thick LiF coating could remarkably improve the cyclability of Li||Li symmetric cells and Li||Cu asymmetric cells, compared to bare cells. In another study,[149] an ALD LiF process had been applied to stitch two-dimensional (2D) h-BN nanocrystals through depositing at their point defects and line defects. The Cu foil coated by the resulting LiF-stitched h-BN film was able to suppress lithium dendrite formation. It enabled more than 300 Li-stripping/plating cycles in Li||Cu cells, which is much better than that of the bare Cu foil, LiF-coated Cu foil, and h-BN-coated Cu foil. Additionally, Li_3PO_4 was investigated as a surface coating of Li metal.[144] It was reported that a 10 nm-thick Li_3PO_4 coating is effective for extending the cyclability of Li||Li cells. Furthermore, the Li_3PO_4-coated Li was coupled with an NCA cathode and the resulting Li||NCA cell exhibited a higher sustainable capacity (125 *vs.* 105 mA h g^{-1} of bare cell) and a higher coulombic efficiency (99.8% *vs.* 92% of bare cell) in 150 charge/discharge cycles and facilitated achieving a higher rate capability. We reported a new ALD process[124] enabling a ternary sulfide compound of LAS through combining two sub-ALD processes of Li_2S[128] and Al_2S_3.[150] In the study, we confirmed that the resulting film in a 1/1 sub-ALD cycle ratio of Li_2S/Al_2S_3 (*i.e.*, 1 : 1 LAS) could achieve an ionic conductivity of 2.5×10^{-7} S cm^{-1} at room temperature. A 50 nm-thick 1 : 1 LAS film was coated onto Li and Cu foils, and the coated Li and Cu foils were then assembled into Li||Li and Li||Cu cells, respectively, for electrochemical evaluations. Using electrochemical impedance spectroscopy (EIS), our measurements revealed that the 1 : 1 LAS coating could stabilize the Li||Li symmetric cells' interface, remarkably reduce the formation SEI, and minimize the EIS. Compared to the bare Li||Li cells, the 1 : 1 LAS-coated Li||Li cells exhibited an impedance 5 times lower after stabilization (Fig. 3a). In addition, we found that the 50 nm-thick 1 : 1 LAS coating on Cu foils could help Li||Cu cells achieve a much better cyclability and much higher sustainable coulombic efficiency (CE) (Fig. 3b). We further revealed that, compared to the evident Li dendrites formed on bare Cu foils (Fig. 3c and e), the 50 nm-thick 1 : 1 LAS coating on the Cu foil prevented the formation of Li dendrites during plating (Fig. 3d and f). By tuning the sub-ALD cycle ratio of Li_2S/Al_2S_3 to 1/4, in a subsequent study we found that the 1 : 4 LAS can achieve a much higher ionic conductivity of 10^{-3} S cm^{-1} at room temperature.[151]

3.2. Organic surface coatings *via* MLD

Following some early efforts by ALD, MLD has also been applied to develop polymeric coatings for addressing the issues of Li metal anodes. In 2018, two independent studies commonly investigated the same alucone AlEG as a new

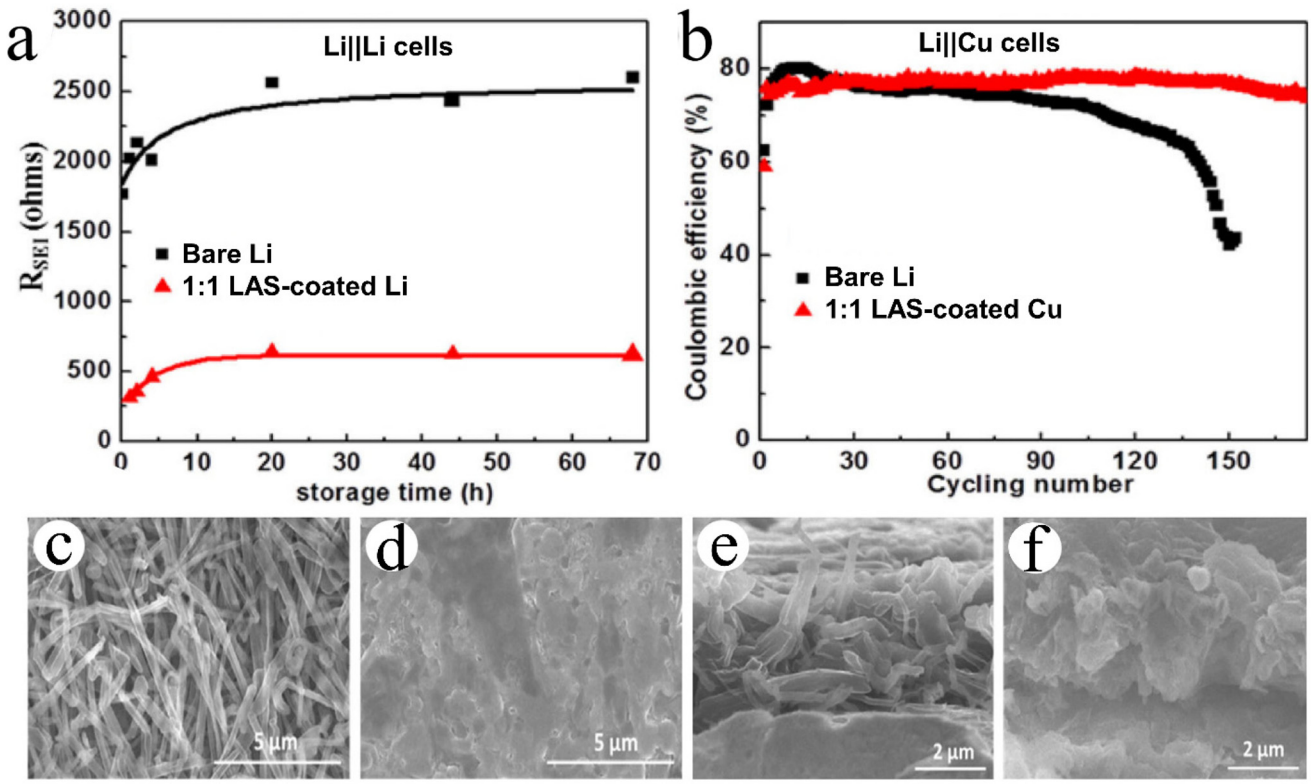

Fig. 3 Effects of ALD Li_xAl_yS on Li metal anodes and Cu current collectors:[124] (a) R_{SEI} of Li/electrolyte/Li symmetric cells *versus* storage time. (b) Coulombic efficiency of Li platting/stripping in 1 M $LiPF_6$ in 3 : 7 EC/EMC (EC = ethylene carbonate and EMC = ethyl methyl carbonate). (c and d) Top-view and (e and f) cross-sectional SEM images of Li metal deposited on (c and e) pristine Cu and (d and f) Cu coated with a 50 nm Li_xAl_yS ALD film. Reprinted (adapted) with permission from ref. 124. Copyright (2016) John Wiley and Sons.

coating over Li metal anodes.[134,152] They applied two different MLD process temperatures: 150 and 120 °C. Chen *et al.*[152] disclosed that, compared to bare Li||Li cells, the symmetric Li||Li cells coated by a 6 nm AlEG coating enabled a much more stable voltage profile. Bare Li||Li cells failed after ~158 h, while the AlEG-coated Li||Li cells survived over 200 h with a gradually increased overpotential. The beneficial effects of AlEG coatings were also revealed in another study by Zhao *et al.*[134] Their optimal coating thickness is ~25 nm. In particular, they comparatively demonstrated that the AlEG coating by MLD is better than that of the Al_2O_3 coating by ALD in improving cell cyclability in Li||Li cells, probably due to the better flexibility of the MLD AlEG coating. Similarly, ZrEG was also studied as a coating of Li metal anodes and it was disclosed that a 4 nm-thick coating could remarkably help improve Li||Li cells' performance.[153]

In addition to the afore-discussed studies on metalcones, there was also a study investigating a pure polymer, polyurea (PU), *via* MLD.[154] In the study, Sun *et al.* deposited PU on Li metal anodes at a GPC of ~0.4 nm per cycle at 65 °C. They reported that a 4 nm-thick PU (10 cycles of the PU MLD process, *i.e.*, Li@P10) could well protect Li metal from corrosion, remarkably extend the cyclability, and stabilize the overpotential of Li||Li cells (Fig. 4a). The PU-modified Li||Li cells could achieve a long cyclability more than 1000 h. Furthermore, they coupled the Li@P10 anode with an LFP cathode and investigated the resulting Li||LFP LMB cells' performance. They revealed that the Li@P10 could help achieve better sustainable capacity (Fig. 4b) and better rate capacity (Fig. 4c–e).

Different from all these afore-discussed studies on Li-free polymeric coatings, we have recently been focusing on develop-

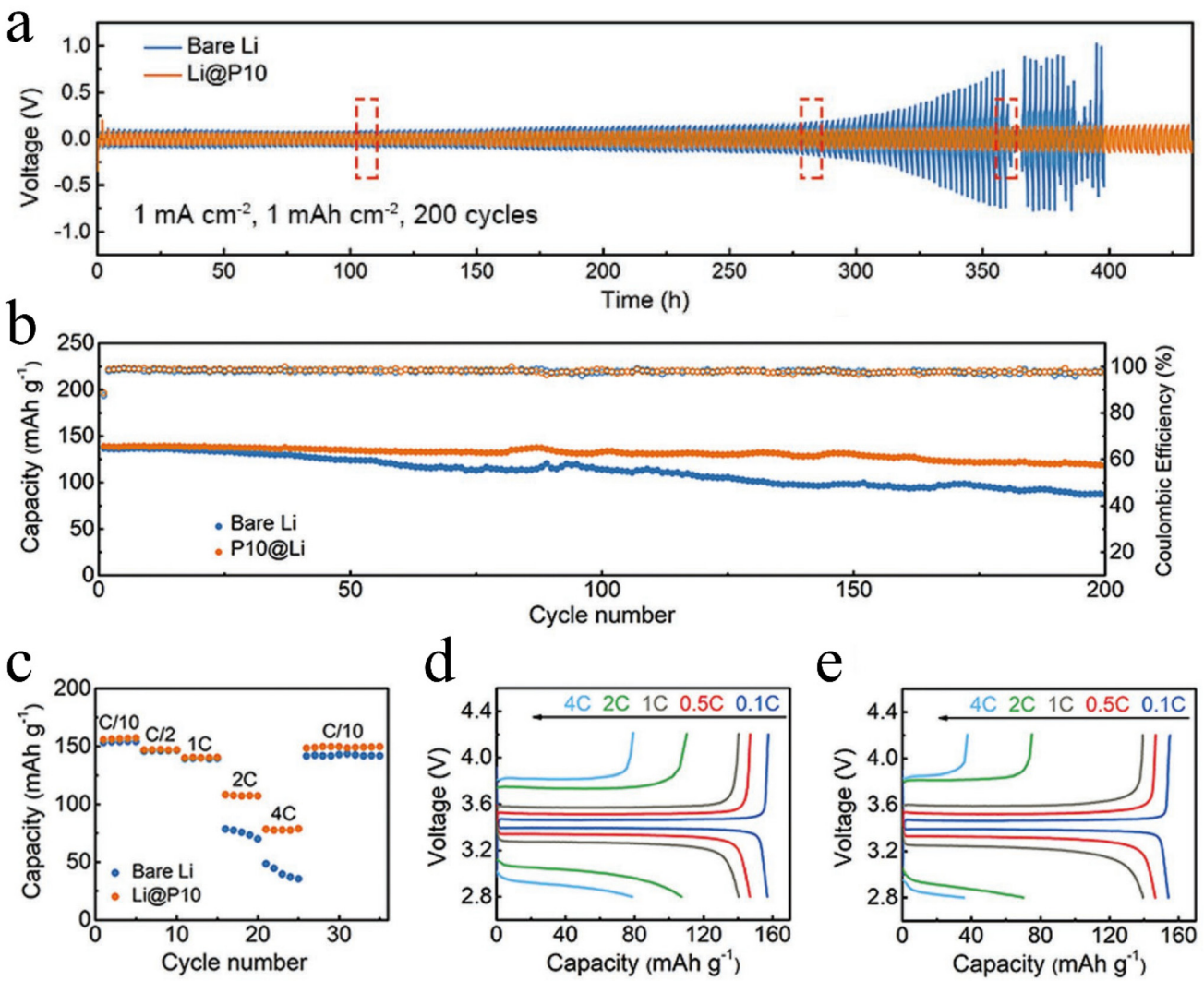

Fig. 4 Effects of MLD polyurea on Li metal anodes:[154] the performance of (a) Li||Li symmetric cells at 1 mA cm^{-2} and 1 mA h cm^{-2} and Li||LFP LMB full cells at (b) a rate of 1C (*i.e.*, 170 mA g^{-1}) and (c) different rates ranging from 0.1 to 4C. Galvanostatic charge/discharge voltage profiles of (d) Li@P10 and (e) bare Li. The electrolyte is 1 M LiPF6 in 1/1/1 volume ratio of EC/DEC/DMC (EC = ethylene carbonate, DEC = diethyl carbonate, and DMC = dimethyl carbonate). Reprinted (adapted) with permission from ref. 154. Copyright (2019) John Wiley and Sons.

ing lithicones, Li-containing polymers, including LiGL (GL = glycerol)[137] and LiTEA (TEA = triethanolamine)[138] reported to date using MLD. Compared to the above-mentioned metalcones and pure polymers, our lithicones endowed much better performance to Li||Li and Li||NMC cells. Particularly, our LiGL MLD exhibited the highest GPC of ~2.7 nm per cycle at 150 °C and could coat graphene nanosheets (GNS) conformally (Fig. 5a–c). This LiGL coating was applied on Li metal anodes with different coating thicknesses by controlling its MLD cycles. The resulting Li metal anodes were named LiGLXX, where XX indicates MLD cycles. For example, LiGL10 signifies the Li metal anodes coated by 10 MLD cycles of LiGL, and so

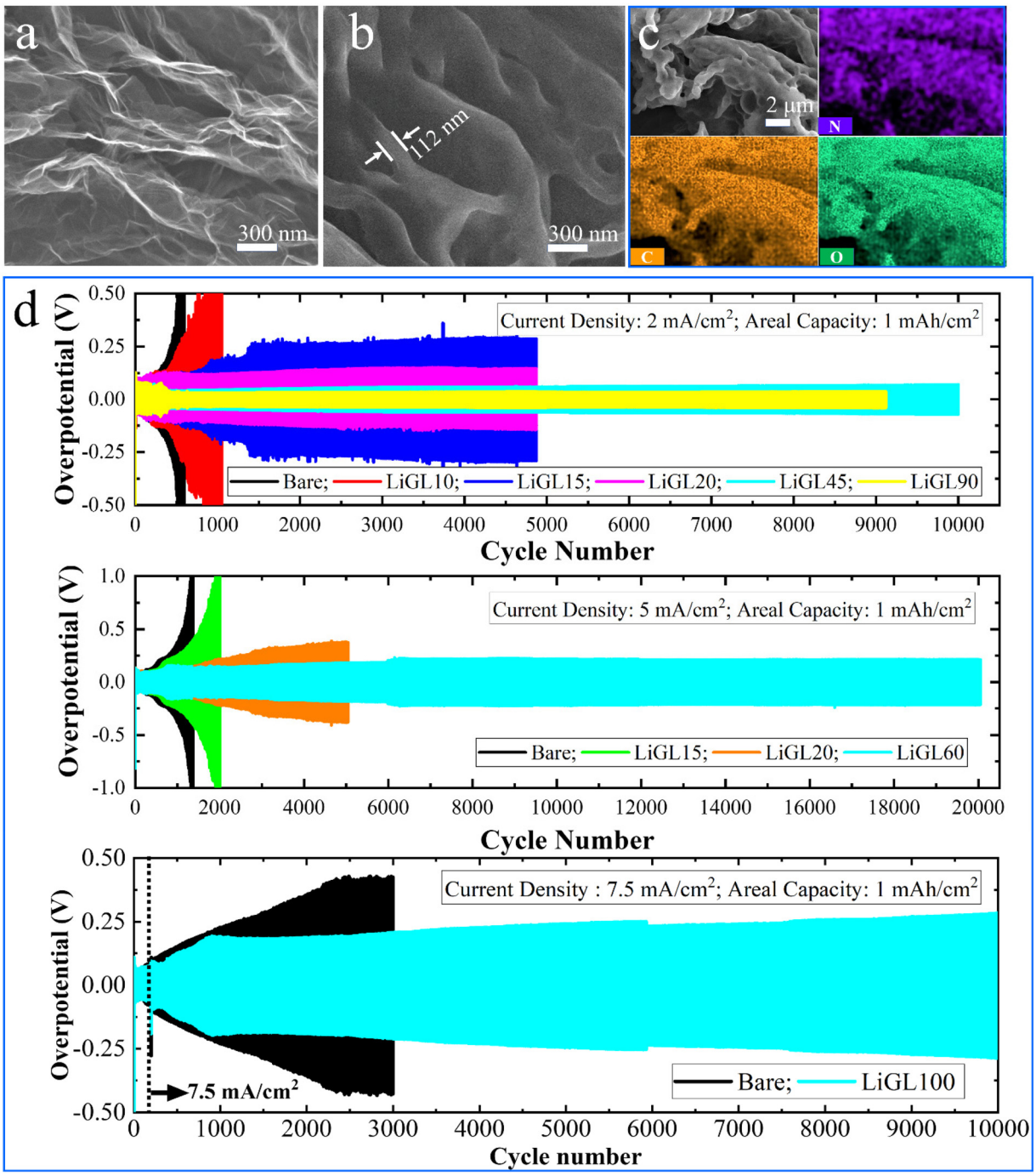

Fig. 5 Effects of MLD LiGL on Li metal anodes:[137] (a) bare GNS, (b) GNS coated by 20-MLD-cycle of LiGL, (c) EDX mapping of LiGL-coated GNS, and (d) effects of LiGL on Li anodes at different current densities (2, 5, and 7.5 mA cm^{-2}) and a fixed areal capacity of 1 mA h cm^{-2}. The electrolyte is 1 M LiTFSI (lithium bis(trifluoromethanesulfonyl)imide) in 1/1 volume ratio of DOL/DME (DOL = 1,3-dioxalane and DME = 1,2-dimethoxyethane). Reprinted (adapted) with permission from ref. 137 under a Creative Commons Attribution (CC BY) license.

forth. Very excitingly, it was for the first time reported that Li metal anodes can be coated with a very thick LiGL film over 200 nm or higher but still achieve a superlong cyclability of over 20000 Li-stripping/plating cycles (over 10000 h) without failures (Fig. 5d). In addition, this LiGL coating can tolerate a high areal current density of up to 7.5 mA cm^{-2} or higher. Impressively, our observation using a scanning electron microscope (SEM) uncovered that the Li metal can be well protected from corrosion (SEI and dendrites) with a sufficiently thick LiGL coating (*e.g.*, LiGL60) (Fig. 6a and b). Our analyses by X-ray photoelectron spectroscopy (XPS) further confirmed that, compared to the thick SEI layer (indicated by the thickness of fluorine (F) from the decomposition of LiTFSI, where LiTFSI used the Li salt in the electrolyte) formed on the bare Li metal after 10 Li-stripping/plating cycles (Fig. 6c), the LiGL90 is SEI-free after 10 (Fig. 6d) and 50 Li-stripping/plating cycles (Fig. 6e). We further studied the exceptional protection effects of the LiGL coating in a novel experiment by performing ultra-long stripping/plating processes for up to 24 h at 2 mA cm^{-2} in Li||Li cells. After a 24 h stripping (Fig. 7a), we noticed many erupted spots on bare Li. These erupted spots were not uniformly distributed. Very strikingly, on the other side, 24 h plating formed a top layer comprising a large number of dendritic structures (Fig. 7b). In sharp contrast, LiGL60 was smooth but decorated with many cracks after 24 h stripping (Fig. 7c) and plating (Fig. 7d). In the study, we confirmed that these cracks are due to the mechanical press during cell assembling but not due to the stripping and plating. These compelling results well verified that the LiGL coating can effectively protect the Li metal from corrosion. Following this stripping/plating process, we subsequently conducted a reverted 24 h plating/stripping process. Again, we confirmed that bare Li anodes suffered from SEI and dendritic growth (Fig. 8a and b), while LiGL60 was nearly intact and did not show any corrosion (Fig. 8c and d). We ascribed the excellent protection of the LiGL coating over Li anodes to its excellent properties, *i.e.*, exceptional ionic conductivity, excellent electrical insulator, good flexibility, and outstanding chemical compatibility and stability. However, we also noticed the cracks of LiGL, indicating that the mechanical properties of LiGL should be further

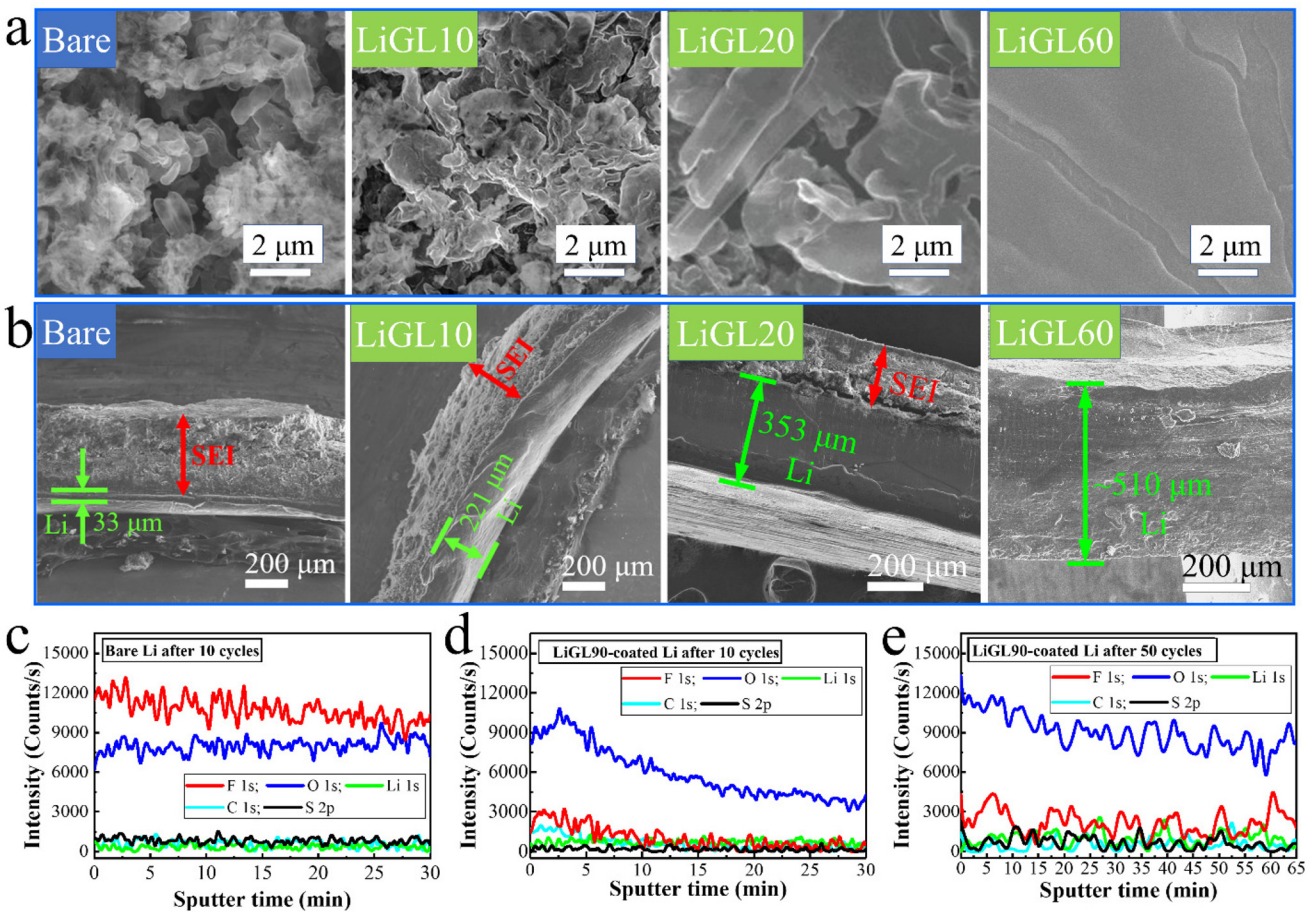

Fig. 6 Analyses on cycled Li||Li cells:[137] SEM images of (a) the surfaces and (b) the cross-sections of the cycled bare, LiGL10, LiGL20, and LiGL60 electrodes after 700 Li-stripping/plating cycles. XPS depth profiling on (c) bare and (d and e) LiGL90 electrodes after (c and d) 10 and (e) 50 Li-stripping/plating cycles. The electrolyte is 1 M LiTFSI in 1/1 volume ratio of DOL/DME. LiGL10, LiGL20, LiGL60, and LiGL90 indicate the LiGL coatings of 10, 20, 60, and 90 MLD cycles, respectively. Reprinted (adapted) with permission from ref. 137 under a Creative Commons Attribution (CC BY) license.

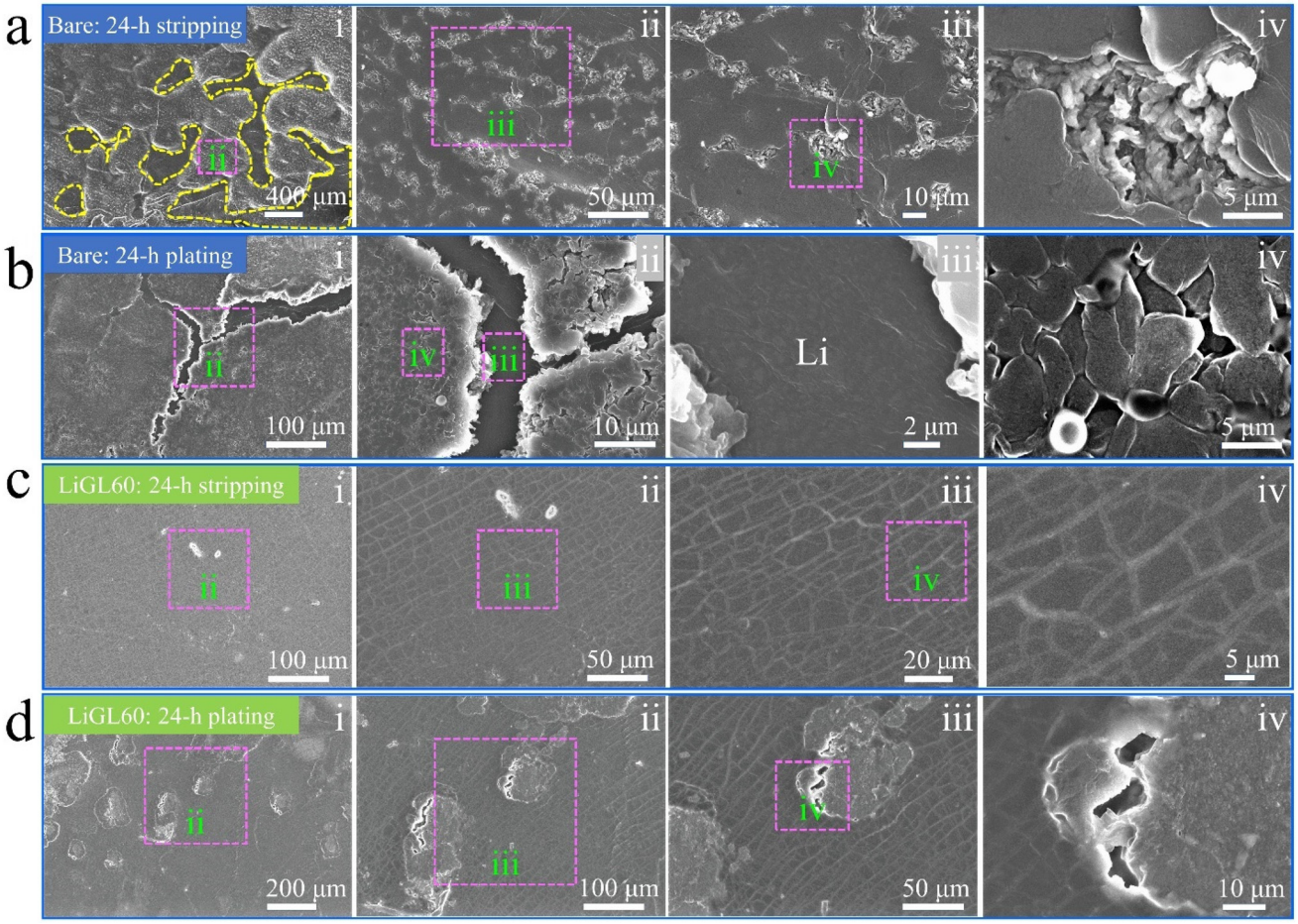

Fig. 7 SEM observations of the morphological changes of Li electrodes:[137] (a and b) bare Li electrode and (c and d) LiGL60 electrode after one 24 h stripping (or plating) at 2 mA cm^{-2}. LiGL60 indicates the LiGL coating of 60 MLD cycles. The electrolyte is 1 M LiTFSI in 1/1 volume ratio of DOL/DME. Reprinted (adapted) with permission from ref. 137 under a Creative Commons Attribution (CC BY) license.

addressed. The excellent protection effects of LiGL have also been further studied for improving Li||NMC LMB cells. The results will be reported somewhere else.

In another recent work,[138] we have reported LiTEA, a new lithicone obtained *via* MLD, which also enables the protection of Li anodes evidently. In Li||Li cells, the LiTEA coating could help achieve a cyclability of over 10000 Li-stripping/plating cycles (>4000 h) without failures at 5 mA cm^{-2} and 1 mA h cm^{-2}. We also confirmed that, protected by a sufficiently thick LiTEA coating (> ~30 nm), an Li anode could avoid forming SEI and growing dendrites. We also demonstrated that Li anodes coated with 200 MLD cycles (~70 nm) of LiTEA (*i.e.*, LiTEA200) can remarkably improve the cyclability of Li||NMC811 (Fig. 9). To couple with NMC811 coated by 20 cycles (~2nm) of ALD Li_2S (*i.e.*, Li_2S20),[155] the resulting LiTEA200||Li_2S20 LMB cells enabled a much better cyclability (Fig. 9a). In addition, we used an energy-dispersive X-ray (EDX) spectrometer to detect the Ni content on the Li anodes after 300 charge/discharge cycles. We found that there are comparable Ni contents on the Li anodes of bare Li||NMC811 and LiTEA200||NMC811 (Fig. 9b and c), but a much lower Ni content on the Li anode of LiTEA200||Li_2S20 (Fig. 9d). This indicates that, to achieve the best cell performance, it would be desirable to tackle the issues of both Li anodes and cathodes together.

3.3. Hybrid surface coatings by ALD and MLD

Not limited to a single coating layer *via* ALD or MLD, very interestingly, Zhao *et al.*[156] have recently developed bilayered hybrid protective films consisting of an MLD-deposited organic layer, alucone (AlEG) and an ALD deposited inorganic layer, Al_2O_3. This combination features tunable layer thickness and property to achieve the optimal protection effects. In Li||Li symmetric cells, they found that 50MLD/50ALD/Li (where "50" is the ALD/MLD cycle number and they were deposited in a bilayered film on Li anodes) performed the best, compared to the 50ALD/50MLD/Li and the bare samples under different testing conditions. Furthermore, the 50MLD/50ALD/Li anodes were used to couple with an S cathode and an LFP cathode in LMB full cells. Compared to the pristine Li foil, the 50MLD/50ALD/Li enabled much better performance for the full cells

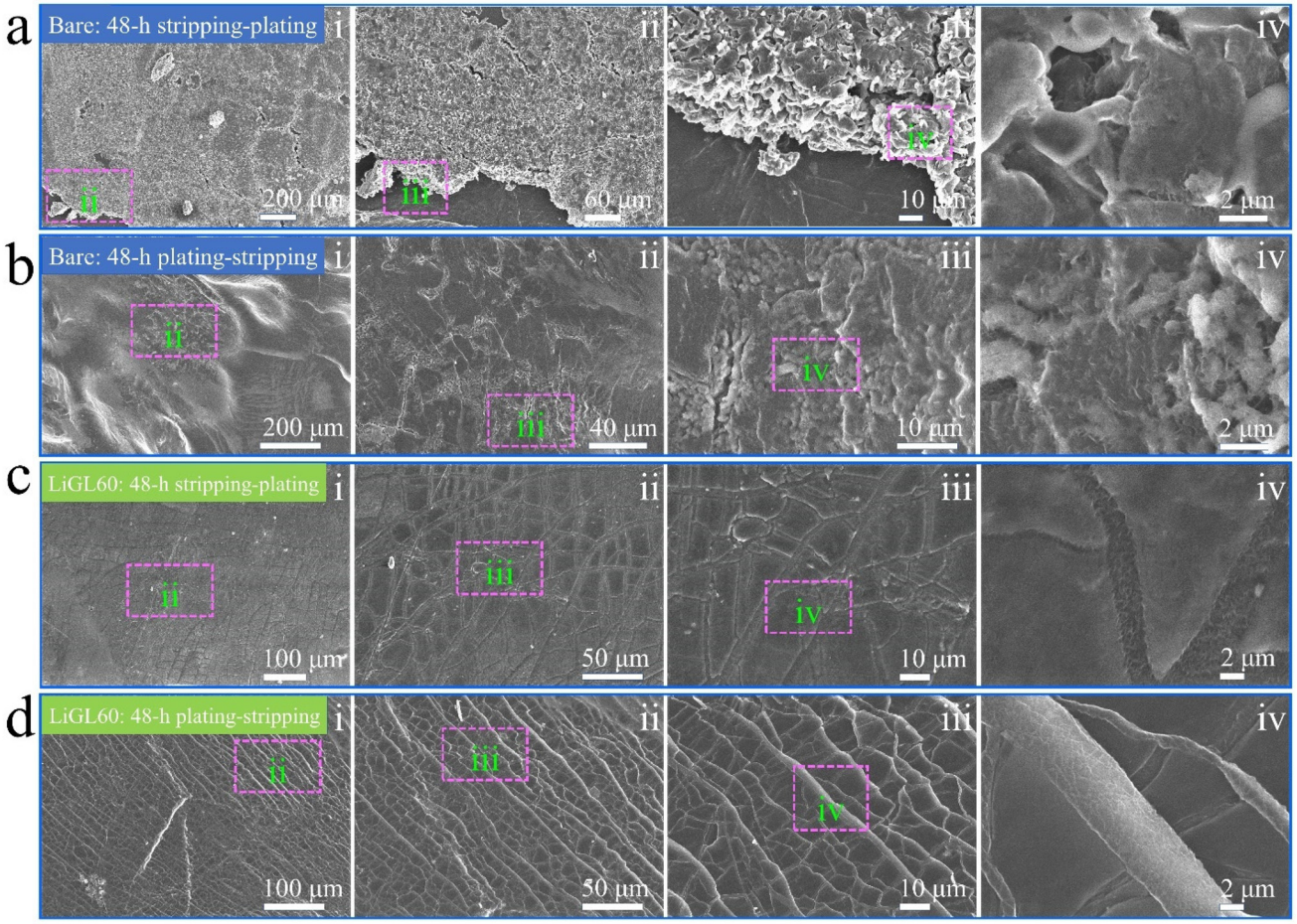

Fig. 8 SEM observations of the morphological changes of Li electrodes:[137] (a and b) bare Li electrode and (c and d) LiGL60 electrode after one 48 h stripping-plating at 2 mA cm^{-2}. LiGL60 indicates the LiGL coating of 60 MLD cycles. The electrolyte is 1 M LiTFSI in 1/1 volume ratio of DOL/DME. Reprinted (adapted) with permission from ref. 137 under a Creative Commons Attribution (CC BY) license.

of Li||S and Li||LFP, in terms of sustainable capacity and cyclability.

4. Tuning lithiophilicity of current collectors

In addition to the afore-discussed protective coatings obtained *via* ALD/MLD, ALD has been applied to modify the current collector-anode interface by growing a thin nucleation layer. The ALD-deposited nucleation layer could tune the Li metal plating morphology for mitigating SEI and dendrite growth.

A copper foil is widely used as the current collector of anodes, including Li metal. Unfortunately, the copper foil exhibits a lithiophobic nature, which presents a high energy barrier for the nucleation of lithium. Such a high nucleation barrier (*i.e.*, overpotential) results in the formation of small and densely distributed lithium particles, increases the contact area with the electrolyte, and thereby leads to the evident formation of SEI, Li dendrites, and cell failure. In addressing these issues, various zero overpotential metallic seeds (Ag and Au) have been studied. Their high costs have prompted researchers to search for cost-effective alternatives. In this regard, we conducted the first study to investigated the effects of 1 : 1 LAS on the performance of Li||Cu cells, in which the 1 : 1 LAS coating was applied on the Cu foil *via* ALD.[124] It was found that 25–50 nm-thick LAS-coated Cu helped Li||Cu cells achieve much longer cyclability (Fig. 3b). In addition, we observed that there were numerous dendritic structures on the pristine Cu foil (Fig. 3c and e), while no dendrites were observed on a 50 nm-thick 1 : 1 LAS-coated Cu after an Li plating process (Fig. 3d and f). In a recent study, Tan *et al.* have studied the effects of TiO_2 nanocoating on the performance of Li||Cu cells.[157] They deposited the TiO_2 coating on the Cu foil with different ALD cycles, while the ALD process has a GPC of 0.8 nm. They revealed that all the ALD TiO_2 coatings of different thicknesses (10, 20, and 30 nm) could help improve the performance of Li||Cu cells, compared to the bare Li||Cu cell. Particularly, the Cu coated with 20 nm-thick TiO_2 (*i.e.*, Cu-20TiO_2) realized the highest CE, the longest cyclability, and the lowest interfacial resistance of the Li||Cu cell. They also noticed that Cu-20TiO_2 lowered the nucleation overpoten-

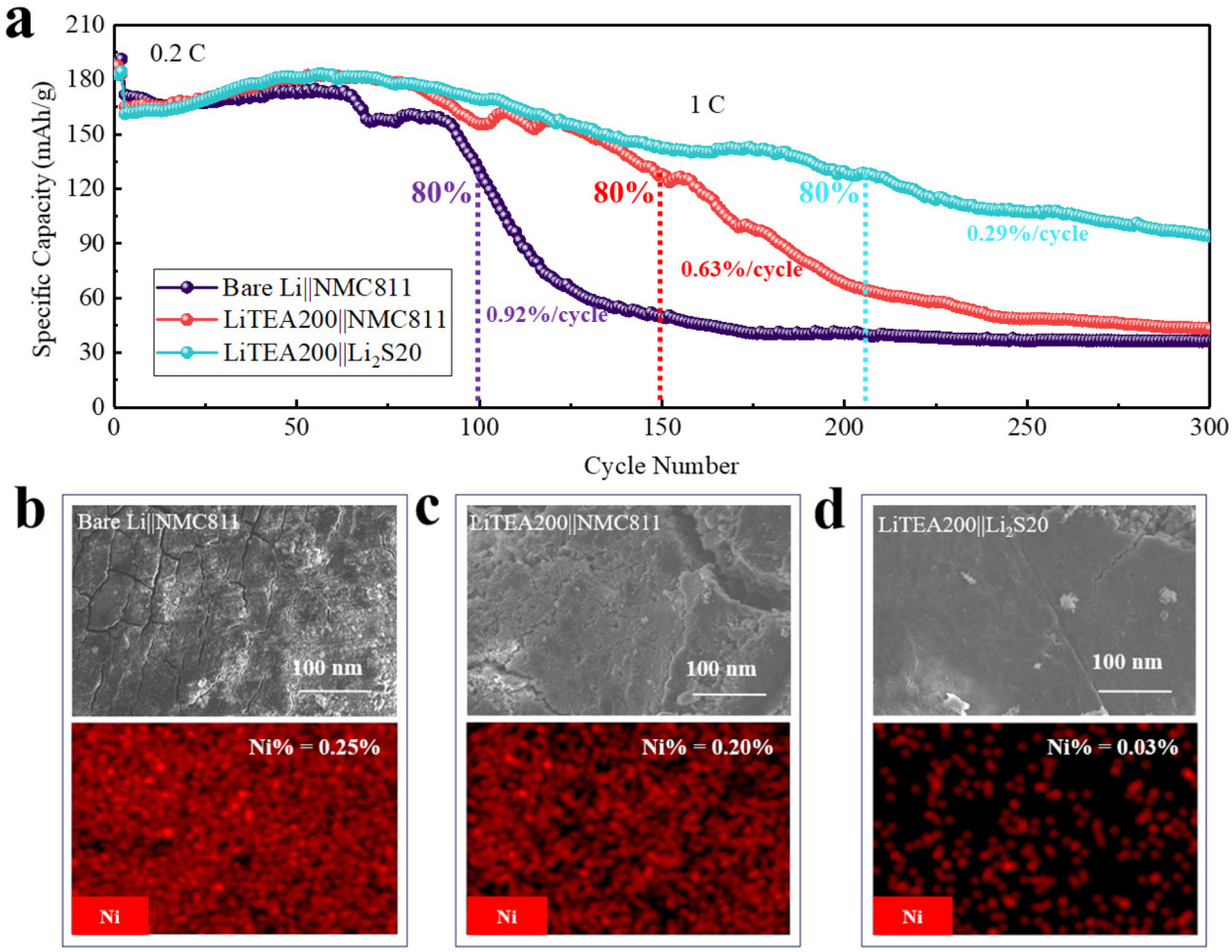

Fig. 9 Effects of ALD Li_2S and MLD LiTEA on the performance of Li||NMC811 LMB cells:[138] (a) cycling performance of Li||NMC full cells. SEM images and EDX mapping of cycled Li electrodes disassembled from (b) bare Li||NMC811, (c) LiTEA200||NMC811, and (d) LiTEA200||Li_2S20 cells. NMC811 is the cathode of $LiNi_{0.8}Mn_{0.1}Co_{0.1}O_2$. LiTEA200 indicates the Li anode with an LiTEA coating of 200 MLD cycles, while Li_2S20 signifies the NMC911 cathode with an Li_2S coating of 20 ALD cycles. All cells were cycled at 1C (1C = 200 mA g^{-1}) for 300 cycles. The electrolyte is 1.2 M $LiPF_6$ in 3/7 weight ratio of EC/EMC. Reprinted (adapted) with permission from ref. 138. Copyright (2023) Elsevier.

tial and voltage hysteresis of the Li||Cu cell (Fig. 10a). Tan *et al.* ascribed these improvements to the better lithiophilicity of Cu-20TiO_2 (due to the 20 nm-thick TiO_2 coating) than that of bare Cu, which could have helped form a more stable and thinner SEI and reduced the energy barrier of Li nucleation. In their study, Tan *et al.* further demonstrated that, through pre-depositing 5 mA h cm^{-2} of Li on the bare Cu and the Cu-20TiO_2, the latter enabled a much better cyclability and a much lower interfacial resistance of Li||LFP full cells (Fig. 10b). The SEM observations revealed that, compared to the pre-deposited Li on the bare Cu (Fig. 10c), the pre-deposited Li on the Cu-20TiO_2 (Fig. 10d) is much denser. After 50 charge/discharge cycles of Li||LFP cells, Li on bare Cu (Fig. 10e) became more porous than Li on Cu-20TiO_2 (Fig. 10f).

In spite of the findings on the beneficial effects of the ALD LAS and TiO_2 coating layers on the improved performance of Li||Cu cells, the afore-discussed studies[124,157] did not provide an in-depth understanding on the underlying mechanism of these coating layers. In this regard, Oyakhire *et al.*[158] conducted an inspiring study and clearly demonstrated that the ALD TiO_2 coating layer could lower the energy barrier of lithium nucleation and thereby help lithium nucleate into larger deposits. Therefore, the deposited Li has a reduced surface area in contact with the electrolyte and forms less SEI, leading to an improved cell performance. Particularly, Oyakhire *et al.*[158] emphasized the importance of ALD for tuning lithophilicity in the following aspects: (1) conformality of the coating layer, (2) scalability at ease, (3) excellent controllability over the coating thickness, and (4) without compromise on cell energy density. In their study, Oyakhire *et al.*[158] also noticed that a nanoscale TiO_2 coating obtained by ALD could dramatically improve the cyclability of Li||Cu cells, while a coating thickness of 5 nm was optimal. Based on lithiation potential curves (inset of Fig. 11a), they found that the nucleation overpotential of lithiation was continuously reduced from

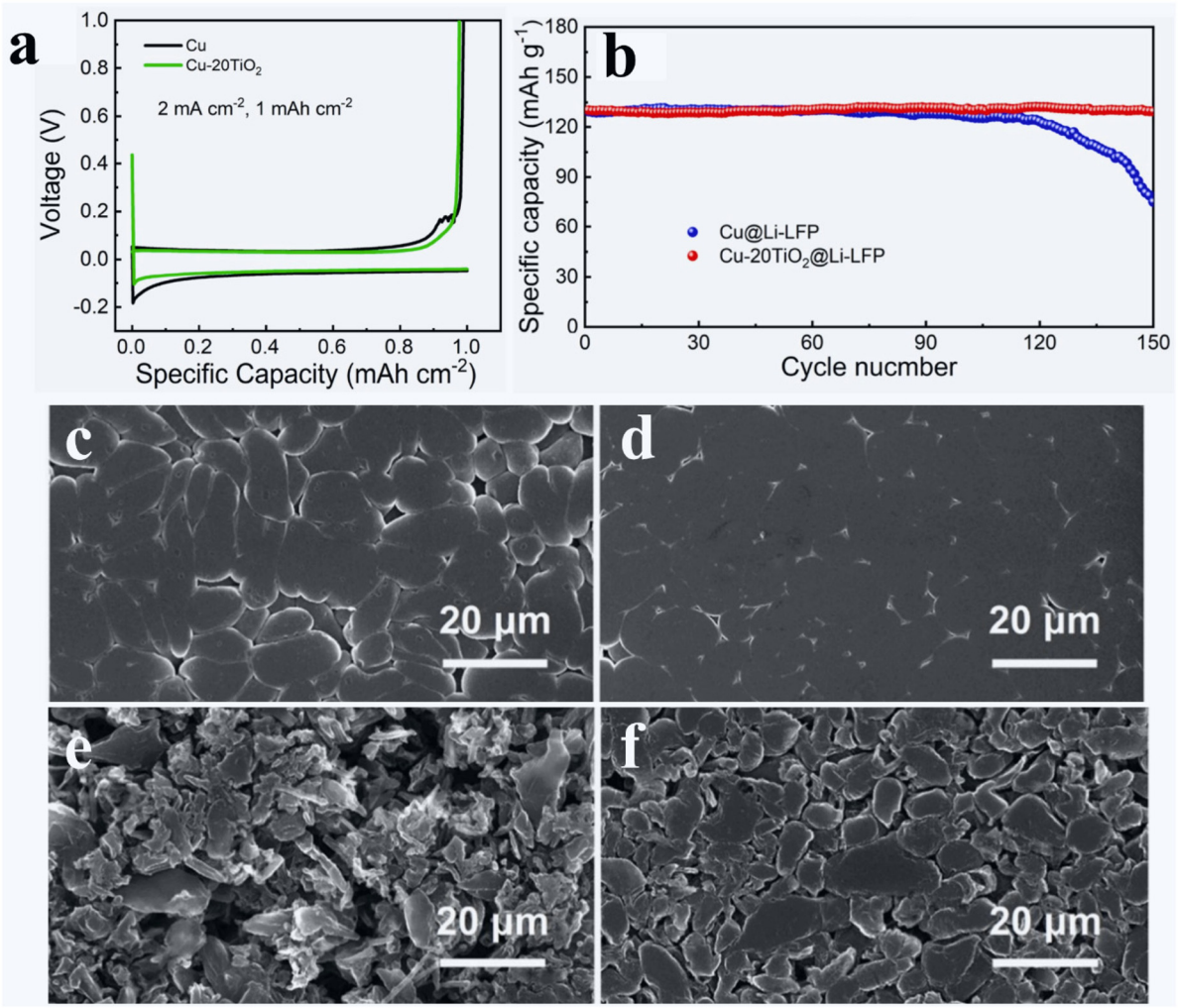

Fig. 10 Effects of ALD TiO_2 on the surface lithiophilicity of the Cu foil:[157] (a) 1st galvanostatic plating/stripping profiles of Cu and Cu-20TiO_2 collectors under 1 mA cm^{-1} and 1 mA h cm^{-2}. (b) Cycling performance of Li||LFP LMB full cells at 1C. SEM images of (c and e) Cu@Li and (d and f) Cu-20TiO_2@Li (c and d) before and (e and f) after 50 charge/discharge cycles in Li||LFP cells. The electrolyte is 1 M LiTFSI in 1/1 volume ratio of DOL/DME with 2 wt% $LiNO_3$. Reprinted (adapted) with permission from ref. 157. Copyright (2020) Elsevier.

129.5 mV on bare Cu to 20.2 mV on the 5 nm-TiO_2 coated Cu with the increase in coating thickness (Fig. 11a). However, a further increase in the TiO_2 coating thickness to 10 nm increased the nucleation overpotential, compared to that of 5 nm TiO_2-coated Cu, probably due to the increased electronic resistance of the coating layer. Very interestingly, Oyakhire *et al.*[158] visualized the morphology of lithium after the first plating under different capacities of 0.1, 0.3, and 1 mA h cm^{-2} but at a fixed current density of 1 mA cm^{-2}. It was revealed that, after a certain capacity (*e.g.*, 0.3 mA h cm^{-2}), there were more isolated small nuclei of lithium on the bare Cu (Fig. 11b), but less large nuclei of lithium on 5 nm TiO_2-coated Cu (Fig. 11c). They believed that the reason lied in the TiO_2 coating layer enabling coalescence of nucleated adatoms and being favorable to the lateral growth of lithium particles. On the contrary, lithium adatoms have poor affinity to bare Cu. After the same capacity of lithium deposition, consequently, the deposited lithium on bare Cu has more exposed surface area and thereby forms more SEI. In comparison, the deposited lithium on the 5 nm TiO_2-coated Cu has less exposed surface area and produces less SEI. Using XPS, Oyakhire *et al.*[158] verified that lithium was deposited on the top of the TiO_2 coating layer. They further probed the lithiophilicity of TiO_2 and noticed a sloping voltage profile with Li||Cu cells using TiO_2-coated Cu (Inset of Fig. 11a). With the increase in the thickness of the TiO_2 layer, particularly, the sloping potential profile increased with an increased capacity. This suggested that some lithium ions have reacted with the TiO_2 layer before lithium nucleation, leading to the production of Li_xTiO_2. They further postulated that the resulting Li_xTiO_2 layer might have favorable wetting properties to lithium and led to larger lithium particles and improved continuity of the plated lithium metal, as illustrated in Fig. 11d.

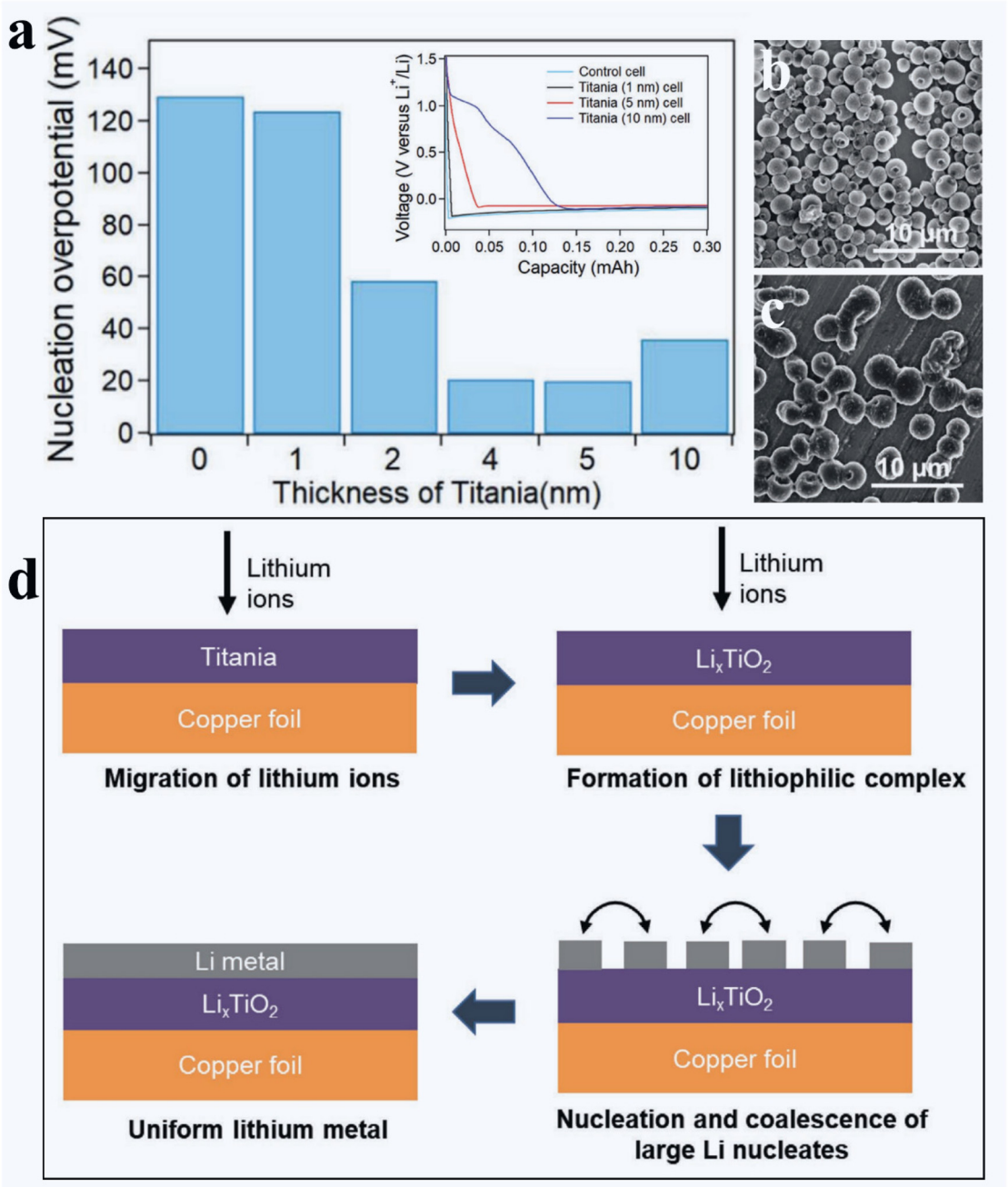

Fig. 11 Effects of ALD TiO_2 on the surface lithiophilicity of the Cu foil.[158] (a) First cycle nucleation overpotential as a function of ALD TiO_2 thickness (inset: voltage profiles for the first cycle of lithium plating for control cell, 1, 5, and 10 nm TiO_2 cells). Top-view SEM images of 0.3 mA h cm^{-2} lithium embryos formed in (b) the control cell and (c) 5 nm TiO_2 cell. (d) Schematic illustration of the role of TiO_2 as a nucleation layer for electrodeposited Li. The electrolyte is 1 M LiTFSI in 1/1 volume ratio of DOL/DME with 1 wt% $LiNO_3$. Reprinted (adapted) with permission from ref. 158. Copyright (2020) John Wiley and Sons.

5. Constituting 3D current collectors

In addition to the surface coatings on planar Li and Cu foils as discussed above, ALD has been applied to modify various 3D porous templates to improve their lithiophilicity. The resulting lithiophilic 3D templates were used as Li hosts in LMB cells for inhibiting SEI and Li dendrite formation. These 3D templates are in general chemically and electrochemically inert and have several functions:[159] (1) provide a constant electrode volume; (2) confine Li within the templates; and (3) reduce local current density to alleviate dendrite growth. ALD coatings play very critical roles for these 3D Li hosts: (1) improve lithiophilicity and (2) enhance the mechanical strength of these Li hosts. The ALD coatings reported to date range from several nanometers to several tens of nanometers.

Liu *et al.*[159] first demonstrated an ALD-modified 3D porous Li host through coating a conformal layer of 30 nm-thick ZnO film over an electrospun polyimide (PI) fiber matrix. The resulting ZnO-coated PI matrix was then put into contact with and covered completely by molten Li. Liu *et al.* verified that molten Li cannot wet the bare PI matrix, while Li reacts with ZnO resulting in the production of an LiZn alloy and Li_2O. The conformal ZnO coating provided the driving force for the molten Li infusion. The resulting Li-coated PI-ZnO matrix was demonstrated to be effective to remarkably improve the cyclability of Li||Li cells and mitigate the cell overpotential. Such a strategy of ALD ZnO was also later practiced on different 3D templates including Cu pillars,[160] carbon fibers,[161,162] and Cu foams (CFs).[163] Using ALD Al_2O_3, this strategy was also applied on a carbon nanotube sponge (CNTS)[164] and cotton.[165] Among these ALD-modified 3D Li hosts, a ZnO-coated hierarchical CF has exhibited compelling effects on the resulting Li||LFP and Li||LCO LMBs.[163] CFs typically have low surface areas. To increase the surface area of a CF (Fig. 12a), Zhang *et al.*[163] first grew $Cu(OH)_2$ nanofibers

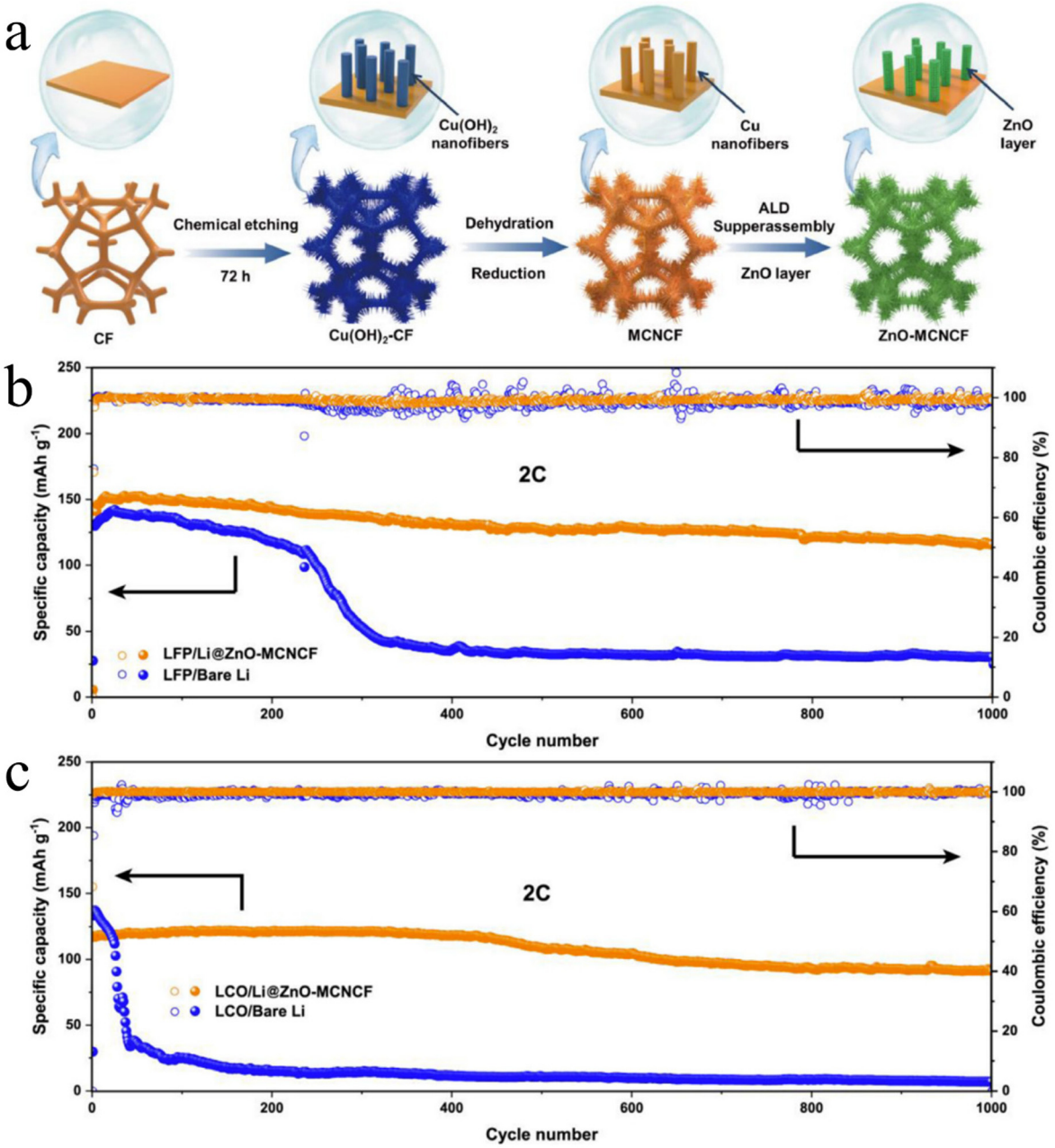

Fig. 12 Effects of ALD ZnO on 3D hierarchical Cu foams:[163] (a) schematic illustration of the preparation process of Zn-MCNCF from CF. Electrochemical performance of (b) Li||LFP and (c) Li||LCO cells due to the adoption of Li@ZnO-MCNCF. The electrolyte is 1 M $LiFP_6$ in 1/1/1 volume ratio of EC/DMC/DEC. Reprinted (adapted) with permission from ref. 163. Copyright (2021) Elsevier.

over a CF (Fig. 12a) *via* a wet chemistry process and then annealed them in a reducing environment to achieve multi-level Cu nanofibers on the CF (MCNCF) (Fig. 12a). The MCNCF was further coated conformally with ZnO *via* ALD (*i.e.*, ZnO-MCNCF) (Fig. 12a). Then, the ZnO-MCNCF was deposited with Li for 10 mA h cm^{-2} at 1 mA cm^{-2} in Li||ZnO-MCNCF cells. Zhang *et al.* found that the Li deposited on the CF (Li@CF) was loose and uneven, while Li deposited on the MCNCF (Li@MCNCF) was uniform but only on the upper layer of the MCNCF. In comparison, the Li deposited on the ZnO-MCNCF (Li@ZnO-MCNCF) was uniform across the ZnO-MCNCF skeleton. The resulting Li@ZnO-MCNCF anodes were used for testing in Li||Li symmetric cells and Li||LFP and Li||LCO full cells. Compared to Li@CF and Li@MCNCF, the Li@ZnO-MCNCF could achieve the longest cyclability with the lowest overpotential in Li||Li cells. Very impressively, the Li@ZnO-MCNCF could achieve very long cyclability (1000 cycles) and very stable sustainable capacities in Li||LFP (Fig. 12b) and Li||LCO (Fig. 12c) LMBs at a high rate of 2 C. This work clearly shows that it is very promising to tackle the issues of Li anodes through adopting suitable measures, while ALD is a very useful technique. Compared to the other 3D Li hosts (Cu pillars,[160] carbon fibers,[161,162] CNTS,[164] and cotton[165]) aided by ALD, this Li@ZnO-MCNCF 3D structure enabled much better electrochemical performance. The underlying mechanisms of the Li@ZnO-MCNCF 3D structure lie in two aspects: (1) excellent lithiophilicity due to the ALD ZnO coating and (2) high specific surface area ascribed to the MCNCF skeleton.

6. Conclusions and outlook

Li metal is the "holy grail" of rechargeable batteries, owing to its highest capacity and lowest potential. The commercialization of Li metal anodes will enable a series of new battery technologies, LMBs, which feature a much higher energy density than that of LIBs. LMBs are highly regarded for addressing the range anxiety of EVs, thereby boosting the EV market. To this end, it is urgent to address the two daunting issues, *i.e.*, continuous SEI formation and dendrite growth. These two issues are two interfacial issues. Thus, interface engineering is very critical for LMBs.

Among various techniques for interface engineering, ALD and MLD are two emerging ones having several unmatched features. Ascribed to their unique growth mechanism and distinctive operation principle, ALD and MLD are granted with a series of unparalleled merits for growing thin films, including exceptional controllability over material growth with atomic and molecular accuracy, low process temperatures, excellent film uniformity and conformality, and unlimited opportunities for new materials. These advantages are essential for ALD and MLD as two novel techniques to practice interface engineering with new solutions in LMBs. First, their low process temperatures make them feasible to deposit films over the Li metal. Second, their viability for inorganic, organic, and hybrid coatings provides an inexhaustible source for searching the most suitable materials with favorable properties to best fulfill interface engineering. Third, their excellent material controllability paves a technical pathway to offer optimal film quality and thickness. Last but not least, their uniformity and conformality are two unrivaled assets for interface engineering of LMBs.

As a consequence, ALD and MLD have to date exhibited three technical pathways for tackling the issues of Li metal anodes: (1) surface coating of Li anodes, (2) tuning lithiophilicity of current collectors, and (3) designing novel 3D Li hosts. In the first place, the effects of surface coatings are highly related to the coatings' properties such as mechanical strength, ionic and electrical conductivity, and chemical and electrochemical stability. In this aspect, desirable coatings *via* ALD and MLD have not been well investigated and there is still a huge space to explore. Our recent studies[124,137,138] for Li-containing organic and inorganic coatings are very compelling and worth some future in-depth studies. Additionally, combining ALD and MLD for hybrid materials is another strategy for novel coatings with desirable properties. To achieve the best performance of Li metal anodes, it may be desirable to have the hybrid coatings made from two excellent organic and inorganic coatings. In the second place, the use of ALD/MLD coatings to tune surface lithiophilicity has not been widely investigated. The studies discussed in this work are still limited. Thus, we would expect more studies to be conducted to disclose the effects of different coatings on lithiophilicity and find zero overpotential coatings with high feasibility technically and financially. In this aspect, only limited ALD coatings have been studied but no MLD coatings have been reported yet. In the third place, limited ALD coatings (ZnO and Al_2O_3) have been applied to modify 3D architecture templates. In the future, it is expected that more ALD/MLD coatings will be investigated. In addition, 3D templates having commercialization potential are preferred.

While we are expecting many more new ALD/MLD coatings with favorable properties to be developed, future studies are also anticipated to evaluate them under much harsher testing conditions (*e.g.*, higher areal current densities and areal capacities, lower and higher temperatures, and different electrolytes). Researchers need to consider the requirements for commercialization. In this respect, the current densities and capacities adopted for testing may not be sufficient for commercialization. Furthermore, it is particularly significant to address the effects of different electrolytes on ALD/MLD coatings. Typically, there are two types of liquid electrolytes used in previous studies, *i.e.*, ether and carbonate, but to date there are less studies in this field. In our studies, we have noticed that the same ALD/MLD coatings may have different effects on the performance of Li metal anodes in different liquid electrolytes. It will be very instructive to uncover the underlying mechanisms. For a certain ALD/MLD coating, one needs to consider the following aspects in order to best practice the coating: (1) its chemical compatibility in different electrolytes and (2) its electrochemical stability with the electrolytes. Not limited to depositing surface coatings in liquid cells, ALD and

MLD are also two powerful tools for rationally designing and developing advanced SEs (iSEs, pSEs, or cSEs). In this respect, we have recently made a comprehensive review on SEs *via* ALD.[15] pSEs and cSEs *via* MLD or/and ALD are currently still at their very early stage. Some Li-containing polymers obtained recently *via* MLD may be promising pSEs.[137,138] They may be combined/mixed with iSEs *via* ALD to form advanced cSEs. Thus, there is still a lot of room for ALD and MLD to boost new battery technologies.

In short, ALD and MLD are two unique tools for practicing interface engineering for LMBs. The studies reported to date in the literature are very interesting, but many more efforts are urgently needed to further advance novel technologies and gain new knowledge for the commercialization of Li metal anodes.

Conflicts of interest

There are no conflicts to declare.

Acknowledgements

We acknowledge partial support from U.S. Department of Energy, Office of Science, Office of Basic Energy Sciences with the award number of DE-SC0023439. We also appreciate partial support from Chancellor Commercialization Fund and Chancellor Gap Fund from the University of Arkansas, Fayetteville, AR, USA.

References

1 A. García-Olivares, J. Solé and O. Osychenko, Transportation in a 100% renewable energy system, *Energy Convers. Manage.*, 2018, **158**, 266–285.
2 Z. W. Seh, Y. Sun, Q. Zhang and Y. Cui, Designing high-energy lithium-sulfur batteries, *Chem. Soc. Rev.*, 2016, **45**(20), 5605–5634.
3 G. Crabtree, E. Kócs and L. Trahey, The energy-storage frontier: Lithium-ion batteries and beyond, *MRS Bull.*, 2015, **40**(12), 1067–1078.
4 M. M. Thackeray, C. Wolverton and E. D. Isaacs, Electrical energy storage for transportation-approaching the limits of, and going beyond, lithium-ion batteries, *Energy Environ. Sci.*, 2012, **5**(7), 7854–7863.
5 S. Zhang, Status, opportunities, and challenges of electrochemical energy storage, *Front. Energy Res.*, 2013, **1**, 8.
6 G. E. Blomgren, The development and future of lithium ion batteries, *J. Electrochem. Soc.*, 2017, **164**(1), A5019–A5025.
7 R. Schmuch, R. Wagner, G. Hörpel, T. Placke and M. Winter, Performance and cost of materials for lithium-based rechargeable automotive batteries, *Nat. Energy*, 2018, **3**(4), 267–278.
8 X.-B. Cheng, J.-Q. Huang and Q. Zhang, Review–Li metal anode in working lithium-sulfur batteries, *J. Electrochem. Soc.*, 2018, **165**(1), A6058–A6072.
9 X.-B. Cheng, R. Zhang, C.-Z. Zhao and Q. Zhang, Toward safe lithium metal anode in rechargeable batteries: A review, *Chem. Rev.*, 2017, **117**(15), 10403–10473.
10 S. Li, M. Jiang, Y. Xie, H. Xu, J. Jia and J. Li, Developing high–performance lithium metal anode in liquid electrolytes: Challenges and progress, *Adv. Mater.*, 2018, **30**(17), 1706375.
11 B. Liu, J.-G. Zhang and W. Xu, Advancing lithium metal batteries, *Joule*, 2018, **2**(5), 833–845.
12 W. Xu, J. Wang, F. Ding, X. Chen, E. Nasybulin, Y. Zhang and J.-G. Zhang, Lithium metal anodes for rechargeable batteries, *Energy Environ. Sci.*, 2014, **7**(2), 513–537.
13 L. Sun, G. Yuan, L. Gao, J. Yang, M. Chhowalla, M. H. Gharahcheshmeh, K. K. Gleason, Y. S. Choi, B. H. Hong and Z. Liu, Chemical vapour deposition, *Nat. Rev. Methods Primers*, 2021, **1**(1), 5.
14 S. Lobe, A. Bauer, S. Uhlenbruck and D. Fattakhova-Rohlfing, Physical Vapor Deposition in Solid-State Battery Development: From Materials to Devices, *Adv. Sci.*, 2021, **8**(11), 2002044.
15 X. Meng, Atomic layer deposition of solid-state electrolytes for next-generation lithium-ion batteries and beyond: Opportunities and challenges, *Energy Storage Mater.*, 2020, **30**, 296–328.
16 X. Meng, Atomic and molecular layer deposition in pursuing better batteries, *J. Mater. Res.*, 2021, **36**, 2–25.
17 X. Meng, X. Q. Yang and X. L. Sun, Emerging applications of atomic layer deposition for lithium-ion battery studies, *Adv. Mater.*, 2012, **24**(27), 3589–3615.
18 Q. Sun, K. C. Lau, D. Geng and X. Meng, Atomic and molecular layer deposition for superior lithium-sulfur batteries: Strategies, performance, and mechanisms, *Batteries Supercaps*, 2018, **1**(2), 41–68.
19 X. Meng, Atomic-scale surface modifications and novel electrode designs for high-performance sodium-ion batteries via atomic layer deposition, *J. Mater. Chem. A*, 2017, **5**, 10127–10149.
20 X. Meng, An overview of molecular layer deposition for organic and organic-inorganic hybrid materials: Mechanisms, growth characteristics, and promising applications, *J. Mater. Chem. A*, 2017, **5**(35), 18326–18378.
21 M. D. Groner, F. H. Fabreguette, J. W. Elam and S. M. George, Low-temperature Al_2O_3 atomic layer deposition, *Chem. Mater.*, 2004, **16**(4), 639–645.
22 R. L. Puurunen, Growth Per Cycle in Atomic Layer Deposition: A Theoretical Model, *Chem. Vap. Deposition*, 2003, **9**(5), 249–257.
23 R. L. Puurunen, Surface chemistry of atomic layer deposition: A case study for the trimethylaluminum/water process, *J. Appl. Phys.*, 2005, **97**(12), 121301.
24 V. Miikkulainen, M. Leskelä, M. Ritala and R. L. Puurunen, Crystallinity of inorganic films grown by

atomic layer deposition: Overview and general trends, *J. Appl. Phys.*, 2013, **113**(2), 021301.
25 R. L. Puurunen, Surface chemistry of atomic layer deposition: A case study for the trimethylaluminum/water process, *J. Appl. Phys.*, 2005, **97**, 121301.
26 H. Zhou and S. F. Bent, Fabrication of organic interfacial layers by molecular layer deposition: Present status and future opportunities, *J. Vac. Sci. Technol., A*, 2013, **31**(4), 040801.
27 H.-I. Shao, S. Umemoto, T. Kikutani and N. Okui, Layer-by-layer polycondensation of nylon 66 by alternating vapour deposition polymerization, *Polymer*, 1997, **38**(2), 459–462.
28 Y. Du and S. M. George, Molecular layer deposition of nylon 66 films examined using in situ FTIR spectroscopy, *J. Phys. Chem. C*, 2007, **111**(24), 8509–8517.
29 T. Yoshimura, S. Tatsuura, W. Sotoyama, A. Matsuura and T. Hayano, Quantum wire and dot formation by chemical vapor deposition and molecular layer deposition of one–dimensional conjugated polymer, *Appl. Phys. Lett.*, 1992, **60**(3), 268–270.
30 T. Yoshimura, A. Oshima, D.-I. Kim and Y. Morita, Quantum dot formation in polymer wires by three-molecule molecular layer deposition (MLD) and applications to electro-optic/photovoltaic devices, *ECS Trans.*, 2009, **25**(4), 15–25.
31 T. Yoshimura, R. Ebihara and A. Oshima, Polymer wires with quantum dots grown by molecular layer deposition of three source molecules for sensitized photovoltaics, *J. Vac. Sci. Technol., A*, 2011, **29**(5), 051510.
32 T. Yoshimura and S. Ishii, Effect of quantum dot length on the degree of electron localization in polymer wires grown by molecular layer deposition, *J. Vac. Sci. Technol., A*, 2013, **31**(3), 031501.
33 A. Kim, M. A. Filler, S. Kim and S. F. Bent, Layer-by-layer growth on Ge(100) via spontaneous urea coupling reactions, *J. Am. Chem. Soc.*, 2005, **127**(16), 6123–6132.
34 P. W. Loscutoff, H. Zhou, S. B. Clendenning and S. F. Bent, Formation of organic nanoscale laminates and blends by molecular layer deposition, *ACS Nano*, 2010, **4**(1), 331–341.
35 H. Zhou and S. F. Bent, Molecular layer deposition of functional thin films for advanced lithographic patterning, *ACS Appl. Mater. Interfaces*, 2011, **3**(2), 505–511.
36 H. Zhou, M. F. Toney and S. F. Bent, Cross-linked ultrathin polyurea films via molecular layer deposition, *Macromolecules*, 2013, **46**(14), 5638–5643.
37 Y.-S. Park, S.-E. Choi, H. Kim and J. S. Lee, Fine-tunable absorption of uniformly aligned polyurea thin films for optical filters using sequentially self-limited molecular layer deposition, *ACS Appl. Mater. Interfaces*, 2016, **8**(18), 11788–11795.
38 N. M. Adamczyk, A. A. Dameron and S. M. George, Molecular layer deposition of poly(p-phenylene terephthalamide) films using terephthaloyl chloride and p-phenylenediamine, *Langmuir*, 2008, **24**(5), 2081–2089.
39 Q. Peng, K. Efimenko, J. Genzer and G. N. Parsons, Oligomer orientation in vapor-molecular-layer-deposited alkyl-aromatic polyamide films, *Langmuir*, 2012, **28**(28), 10464–10470.
40 S. E. Atanasov, M. D. Losego, B. Gong, E. Sachet, J.-P. Maria, P. S. Williams and G. N. Parsons, Highly conductive and conformal poly(3,4-ethylenedioxythiophene) (PEDOT) thin films via oxidative molecular layer deposition, *Chem. Mater.*, 2014, **26**(11), 3471–3478.
41 D. H. Kim, S. E. Atanasov, P. Lemaire, K. Lee and G. N. Parsons, Platinum-free cathode for dye-sensitized solar cells using poly(3,4-ethylenedioxythiophene) (PEDOT) formed via oxidative molecular layer deposition, *ACS Appl. Mater. Interfaces*, 2015, **7**(7), 3866–3870.
42 T. Miyamae, K. Tsukagoshi, O. Matsuoka, S. Yamamoto and H. Nozoye, Preparation of polyimide-polyamide random copolymer thin film by sequential vapor deposition polymerization, *Jpn. J. Appl. Phys.*, 2002, **41**(2R), 746.
43 P. W. Loscutoff, H.-B.-R. Lee and S. F. Bent, Deposition of ultrathin polythiourea films by molecular layer deposition, *Chem. Mater.*, 2010, **22**(19), 5563–5569.
44 T. V. Ivanova, P. S. Maydannik and D. C. Cameron, Molecular layer deposition of polyethylene terephthalate thin films, *J. Vac. Sci. Technol., A*, 2012, **30**(1), 01A121.
45 Y.-H. Li, D. Wang and J. M. Buriak, Molecular layer deposition of thiol–ene multilayers on semiconductor surfaces, *Langmuir*, 2010, **26**(2), 1232–1238.
46 S. A. Vasudevan, Y. Xu, S. Karwal, H. G. M. E. van Ostaay, G. M. H. Meesters, M. Talebi, E. J. R. Sudholter and J. Ruud van Ommen, Controlled release from protein particles encapsulated by molecular layer deposition, *Chem. Commun.*, 2015, **51**(63), 12540–12543.
47 A. A. Dameron, D. Seghete, B. B. Burton, S. D. Davidson, A. S. Cavanagh, J. A. Bertrand and S. M. George, Molecular layer deposition of alucone polymer films using trimethylaluminum and ethylene glycol, *Chem. Mater.*, 2008, **20**(10), 3315–3326.
48 D. Choudhury, S. K. Sarkar and N. Mahuli, Molecular layer deposition of alucone films using trimethylaluminum and hydroquinone, *J. Vac. Sci. Technol., A*, 2015, **33**(1), 01A115.
49 M. Vähä-Nissi, J. Sievänen, E. Salo, P. Heikkilä, E. Kenttä, L.-S. Johansson, J. T. Koskinen and A. Harlin, Atomic and molecular layer deposition for surface modification, *J. Solid State Chem.*, 2014, **214**, 7–11.
50 X. Liang, D. M. King, P. Li, S. M. George and A. W. Weimer, Nanocoating hybrid polymer films on large quantities of cohesive nanoparticles by molecular layer deposition, *AIChE J.*, 2009, **55**(4), 1030–1039.
51 D. Seghete, B. D. Davidson, R. A. Hall, Y. J. Chang, V. M. Bright and S. M. George, Sacrificial layers for air gaps in NEMS using alucone molecular layer deposition, *Sens. Actuators, A*, 2009, **155**(1), 8–15.
52 D. C. Miller, R. R. Foster, S.-H. Jen, J. A. Bertrand, D. Seghete, B. Yoon, Y.-C. Lee, S. M. George and

M. L. Dunn, Thermomechanical properties of aluminum alkoxide (alucone) films created using molecular layer deposition, *Acta Mater.*, 2009, **57**(17), 5083–5092.

53 X. Liang, M. Yu, J. Li, Y.-B. Jiang and A. W. Weimer, Ultra-thin microporous-mesoporous metal oxide films prepared by molecular layer deposition (MLD), *Chem. Commun.*, 2009, (46), 7140–7142.

54 Y. Qin, Y. Yang, R. Scholz, E. Pippel, X. Lu and M. Knez, Unexpected Oxidation Behavior of Cu Nanoparticles Embedded in Porous Alumina Films Produced by Molecular Layer Deposition, *Nano Lett.*, 2011, **11**(6), 2503–2509.

55 B. H. Lee, B. Yoon, V. R. Anderson and S. M. George, Alucone Alloys with Tunable Properties Using Alucone Molecular Layer Deposition and Al_2O_3 Atomic Layer Deposition, *J. Phys. Chem. C*, 2012, **116**(5), 3250–3257.

56 S.-H. Jen, B. H. Lee, S. M. George, R. S. McLean and P. F. Carcia, Critical tensile strain and water vapor transmission rate for nanolaminate films grown using Al_2O_3 atomic layer deposition and alucone molecular layer deposition, *Appl. Phys. Lett.*, 2012, **101**(23), 234103.

57 J. J. Brown, R. A. Hall, P. E. Kladitis, S. M. George and V. M. Bright, Molecular layer deposition on carbon nanotubes, *ACS Nano*, 2013, **7**(9), 7812–7823.

58 A. J. Loebl, C. J. Oldham, C. K. Devine, B. Gong, S. E. Atanasov, G. N. Parsons and P. S. Fedkiw, Solid Electrolyte Interphase on Lithium-Ion Carbon Nanofiber Electrodes by Atomic and Molecular Layer Deposition, *J. Electrochem. Soc.*, 2013, **160**(11), A1971–A1978.

59 X. Li, A. Lushington, J. Liu, R. Li and X. Sun, Superior stable sulfur cathodes of Li-S batteries enabled by molecular layer deposition, *Chem. Commun.*, 2014, **50**(68), 9757–9760.

60 A. Lushington, J. Liu, M. N. Bannis, B. Xiao, S. Lawes, R. Li and X. Sun, A novel approach in controlling the conductivity of thin films using molecular layer deposition, *Appl. Surf. Sci.*, 2015, **357**(Part B), 1319–1324.

61 J. W. DuMont and S. M. George, Pyrolysis of Alucone Molecular Layer Deposition Films Studied Using In Situ Transmission Fourier Transform Infrared Spectroscopy, *J. Phys. Chem. C*, 2015, **119**(26), 14603–14612.

62 A. I. Abdulagatov, K. E. Terauds, J. J. Travis, A. S. Cavanagh, R. Raj and S. M. George, Pyrolysis of titanicone molecular layer deposition films as precursors for conducting TiO_2/carbon composite films, *J. Phys. Chem. C*, 2013, **117**(34), 17442–17450.

63 Y.-S. Park, H. Kim, B. Cho, C. Lee, S.-E. Choi, M. M. Sung and J. S. Lee, Intramolecular and Intermolecular Interactions in Hybrid Organic–Inorganic Alucone Films Grown by Molecular Layer Deposition, *ACS Appl. Mater. Interfaces*, 2016, **8**(27), 17489–17498.

64 N. Bahlawane, D. Arl, J.-S. Thomann, N. Adjeroud, K. Menguelti and D. Lenoble, Molecular layer deposition of amine-containing alucone thin films, *Surf. Coat. Technol.*, 2013, **230**, 101–105.

65 P. C. Lemaire, C. J. Oldham and G. N. Parsons, Rapid visible color change and physical swelling during water exposure in triethanolamine-metalcone films formed by molecular layer deposition, *J. Vac. Sci. Technol., A*, 2016, **34**(1), 01A134.

66 B. Gong, Q. Peng and G. N. Parsons, Conformal organic–-inorganic hybrid network polymer thin films by molecular layer deposition using trimethylaluminum and glycidol, *J. Phys. Chem. B*, 2011, **115**(19), 5930–5938.

67 C. J. Oldham, B. Gong, J. C. Spagnola, J. S. Jur, K. J. Senecal, T. A. Godfrey and G. N. Parsons, Encapsulation and Chemical Resistance of Electrospun Nylon Nanofibers Coated Using Integrated Atomic and Molecular Layer Deposition, *J. Electrochem. Soc.*, 2011, **158**(9), D549–D556.

68 Y. Lee, B. Yoon, A. S. Cavanagh and S. M. George, Molecular layer deposition of aluminum alkoxide polymer films using trimethylaluminum and glycidol, *Langmuir*, 2011, **27**(24), 15155–15164.

69 B. Gong, J. C. Spagnola and G. N. Parsons, Hydrophilic mechanical buffer layers and stable hydrophilic finishes on polydimethylsiloxane using combined sequential vapor infiltration and atomic/molecular layer deposition, *J. Vac. Sci. Technol., A*, 2012, **30**(1), 01A156.

70 B. Gong and G. N. Parsons, Caprolactone ring-opening molecular layer deposition of organic-aluminum oxide polymer films, *ECS J. Solid State Sci. Technol.*, 2012, **1**(4), P210–P215.

71 D. M. Piper, J. J. Travis, M. Young, S.-B. Son, S. C. Kim, K. H. Oh, S. M. George, C. Ban and S.-H. Lee, Reversible high-capacity Si nanocomposite anodes for lithium-ion batteries enabled by molecular layer deposition, *Adv. Mater.*, 2014, **26**(10), 1596–1601.

72 W. Zhou, J. Leem, I. Park, Y. Li, Z. Jin and Y.-S. Min, Charge trapping behavior in organic-inorganic alloy films grown by molecular layer deposition from trimethylaluminum, p-phenylenediamine and water, *J. Mater. Chem.*, 2012, **22**(45), 23935–23943.

73 B. Yoon, D. Seghete, A. S. Cavanagh and S. M. George, Molecular layer deposition of hybrid organic–inorganic alucone polymer films using a three-step ABC reaction sequence, *Chem. Mater.*, 2009, **21**(22), 5365–5374.

74 D. Seghete, R. A. Hall, B. Yoon and S. M. George, Importance of trimethylaluminum diffusion in three-step ABC molecular layer deposition using trimethylaluminum, ethanolamine, and maleic anhydride, *Langmuir*, 2010, **26**(24), 19045–19051.

75 X. Liang, B. W. Evanko, A. Izar, D. M. King, Y.-B. Jiang and A. W. Weimer, Ultrathin highly porous alumina films prepared by alucone ABC molecular layer deposition (MLD), *Microporous Mesoporous Mater.*, 2013, **168**, 178–182.

76 T. D. Gould, A. Izar, A. W. Weimer, J. L. Falconer and J. W. Medlin, Stabilizing Ni catalysts by molecular layer deposition for harsh, dry reforming conditions, *ACS Catal.*, 2014, **4**(8), 2714–2717.

77 Q. Peng, B. Gong, R. M. VanGundy and G. N. Parsons, "Zincone" zinc oxide–organic hybrid polymer thin films formed by molecular layer deposition, *Chem. Mater.*, 2009, **21**(5), 820–830.

78 B. Yoon, B. H. Lee and S. M. George, Molecular layer deposition of flexible, transparent and conductive hybrid organic-inorganic thin films, *ECS Trans.*, 2011, **41**(2), 271–277.
79 B. Yoon, B. H. Lee and S. M. George, Highly conductive and transparent hybrid organic–inorganic zincone thin films using atomic and molecular layer deposition, *J. Phys. Chem. C*, 2012, **116**(46), 24784–24791.
80 B. Yoon, Y. Lee, A. Derk, C. Musgrave and S. George, Molecular layer deposition of conductive hybrid organic-inorganic thin films using diethylzinc and hydroquinone, *ECS Trans.*, 2011, **33**(27), 191–195.
81 J. Huang, A. T. Lucero, L. Cheng, H. J. Hwang, M.-W. Ha and J. Kim, Hydroquinone-ZnO nano-laminate deposited by molecular-atomic layer deposition, *Appl. Phys. Lett.*, 2015, **106**(12), 123101.
82 J. Huang, H. Zhang, A. Lucero, L. Cheng, S. Kc, J. Wang, J. Hsu, K. Cho and J. Kim, Organic-inorganic hybrid semiconductor thin films deposited using molecular-atomic layer deposition (MALD), *J. Mater. Chem. C*, 2016, **4**(12), 2382–2389.
83 K. S. Han and M. M. Sung, Molecular layer deposition of organic–inorganic hybrid films using diethylzinc and trihydroxybenzene, *J. Nanosci. Nanotechnol.*, 2014, **14**(8), 6137–6142.
84 S. Cho, G. Han, K. Kim and M. M. Sung, High-performance two-dimensional polydiacetylene with a hybrid inorganic–organic structure, *Angew. Chem., Int. Ed.*, 2011, **50**(12), 2742–2746.
85 B. Yoon, J. L. O'Patchen, D. Seghete, A. S. Cavanagh and S. M. George, Molecular layer deposition of hybrid organic-inorganic polymer films using diethylzinc and ethylene glycol, *Chem. Vap. Deposition*, 2009, **15**(4–6), 112–121.
86 C. Chen, P. Li, G. Wang, Y. Yu, F. Duan, C. Chen, W. Song, Y. Qin and M. Knez, Nanoporous nitrogen-doped titanium dioxide with excellent photocatalytic activity under visible light irradiation produced by molecular layer deposition, *Angew. Chem., Int. Ed.*, 2013, **52**(35), 9196–9200.
87 K. Van de Kerckhove, F. Mattelaer, J. Dendooven and C. Detavernier, Molecular layer deposition of "vanadicone", a vanadium-based hybrid material, as an electrode for lithium-ion batteries, *Dalton Trans.*, 2017, **46**, 4542–4553.
88 B. H. Lee, V. R. Anderson and S. M. George, Molecular layer deposition of zircone and ZrO_2/zircone alloy films: growth and properties, *Chem. Vap. Deposition*, 2013, **19**(4–6), 204–212.
89 R. A. Hall, S. M. George, Y. Kim, W. Hwang, M. E. Samberg, N. A. Monteiro-Riviere and R. J. Narayan, Growth of zircone on nanoporous alumina using molecular layer deposition, *JOM*, 2014, **66**(4), 649–653.
90 B. H. Lee, V. R. Anderson and S. M. George, Growth and properties of hafnicone and HfO_2/hafnicone nanolaminate and alloy films using molecular layer deposition techniques, *ACS Appl. Mater. Interfaces*, 2014, **6**(19), 16880–16887.
91 O. Nilsen, K. R. Haug, T. Finstad and H. Fjellvåg, Molecular Hybrid Structures by Atomic Layer Deposition – Deposition of Alq_3, Znq_2 and Tiq_4 (q=8-hydroxyquinoline), *Chem. Vap. Deposition*, 2013, **19**(4–6), 174–179.
92 A. Räupke, F. Albrecht, J. Maibach, A. Behrendt, A. Polywka, R. Heiderhoff, J. Helzel, T. Rabe, H.-H. Johannes, W. Kowalsky, E. Mankel, T. Mayer, P. Görrn and T. Riedl, Conformal and highly luminescent monolayers of Alq_3 prepared by gas-phase molecular layer deposition, *ACS Appl. Mater. Interfaces*, 2014, **6**(2), 1193–1199.
93 L. D. Salmi, M. J. Heikkilä, E. Puukilainen, T. Sajavaara, D. Grosso and M. Ritala, Studies on atomic layer deposition of MOF-5 thin films, *Microporous Mesoporous Mater.*, 2013, **182**, 147–154.
94 L. D. Salmi, M. J. Heikkilä, M. Vehkamäki, E. Puukilainen, M. Ritala and T. Sajavaara, Studies on atomic layer deposition of IRMOF-8 thin films, *J. Vac. Sci. Technol., A*, 2015, **33**(1), 01A121.
95 E. Ahvenniemi and M. Karppinen, Atomic/molecular layer deposition: a direct gas-phase route to crystalline metal-organic framework thin films, *Chem. Commun.*, 2016, **52**(6), 1139–1142.
96 M. Nisula and M. Karppinen, Atomic/molecular layer deposition of lithium terephthalate thin films as high rate capability Li-ion battery anodes, *Nano Lett.*, 2016, **16**(2), 1276–1281.
97 C.-Y. Kao, J.-W. Yoo, Y. Min and A. J. Epstein, Molecular layer deposition of an organic-based magnetic semiconducting laminate, *ACS Appl. Mater. Interfaces*, 2012, **4**(1), 137–141.
98 C.-Y. Kao, B. Li, Y. Lu, J.-W. Yoo and A. J. Epstein, Thin films of organic-based magnetic materials of vanadium and cobalt tetracyanoethylene by molecular layer deposition, *J. Mater. Chem. C*, 2014, **2**(30), 6171–6176.
99 B. Zhang, Y. Chen, J. Li, E. Pippel, H. Yang, Z. Gao and Y. Qin, High efficiency Cu-ZnO hydrogenation catalyst: the tailoring of Cu-ZnO interface sites by molecular layer deposition, *ACS Catal.*, 2015, **5**(9), 5567–5573.
100 T. Tynell, H. Yamauchi and M. Karppinen, Hybrid inorganic–organic superlattice structures with atomic layer deposition/molecular layer deposition, *J. Vac. Sci. Technol., A*, 2014, **32**(1), 01A105.
101 T. Tynell and M. Karppinen, ZnO: Hydroquinone superlattice structures fabricated by atomic/molecular layer deposition, *Thin Solid Films*, 2014, **551**, 23–26.
102 B. H. Lee, M. K. Ryu, S.-Y. Choi, K.-H. Lee, S. Im and M. M. Sung, Rapid vapor-phase fabrication of organic–-inorganic hybrid superlattices with monolayer precision, *J. Am. Chem. Soc.*, 2007, **129**(51), 16034–16041.
103 S. H. Cha, M. S. Oh, K. H. Lee, S. Im, B. H. Lee and M. M. Sung, Electrically stable low voltage ZnO transistors with organic/inorganic nanohybrid dielectrics, *Appl. Phys. Lett.*, 2008, **92**(2), 023506.
104 K. H. Lee, J.-M. Choi, S. Im, B. H. Lee, K. K. Im, M. M. Sung and S. Lee, Low-voltage-driven pentacene

thin-film transistor with an organic-inorganic nanohybrid dielectric, *Appl. Phys. Lett.*, 2007, **91**(12), 123502.

105 B. H. Lee, K. H. Lee, S. Im and M. M. Sung, Vapor-phase molecular layer deposition of self-assembled multilayers for organic thin-film transistor, *J. Nanosci. Nanotechnol.*, 2009, **9**(12), 6962–6967.

106 J. Huang, M. Lee, A. Lucero and J. Kim, Organic-Inorganic Hybrid Nano-laminates Fabricated by Ozone-assisted Molecular-atomic Layer Deposition, *Chem. Vap. Deposition*, 2013, **19**(4–6), 142–148.

107 J. Huang, M. Lee, A. T. Lucero, L. Cheng, M.-W. Ha and J. Kim, 7-Octenyltrichrolosilane/trimethyaluminum hybrid dielectrics fabricated by molecular-atomic layer deposition on ZnO thin film transistors, *Jpn. J. Appl. Phys.*, 2016, **55**(6S1), 06GK04.

108 B. H. Lee, K. K. Im, K. H. Lee, S. Im and M. M. Sung, Molecular layer deposition of ZrO_2-based organic–inorganic nanohybrid thin films for organic thin film transistors, *Thin Solid Films*, 2009, **517**(14), 4056–4060.

109 M. Putkonen and L. Niinistö, Atomic layer deposition of B_2O_3 thin films at room temperature, *Thin Solid Films*, 2006, **514**(1–2), 145–149.

110 T. Jurca, M. J. Moody, A. Henning, J. D. Emery, B. Wang, J. M. Tan, T. L. Lohr, L. J. Lauhon and T. J. Marks, Low-temperature atomic layer deposition of MoS_2 films, *Angew. Chem., Int. Ed.*, 2017, **56**(18), 4991–4995.

111 D. J. Hagen, L. Mai, A. Devi, J. Sainio and M. Karppinen, Atomic/molecular layer deposition of Cu–organic thin films, *Dalton Trans.*, 2018, **47**(44), 15791–15800.

112 S. A. Skoog, J. W. Elam and R. J. Narayan, Atomic layer deposition: Medical and biological applications, *Int. Mater. Rev.*, 2013, **58**(2), 113–129.

113 A. W. Ott, J. W. Klaus, J. M. Johnson and S. M. George, Al3O3 thin film growth on Si(100) using binary reaction sequence chemistry, *Thin Solid Films*, 1997, **292**(1), 135–144.

114 A. Paranjpe, S. Gopinath, T. Omstead and R. Bubber, Atomic Layer Deposition of AlOx for Thin Film Head Gap Applications, *J. Electrochem. Soc.*, 2001, **148**(9), G465–G471.

115 A. W. Ott, K. C. McCarley, J. W. Klaus, J. D. Way and S. M. George, Atomic layer controlled deposition of Al_2O_3 films using binary reaction sequence chemistry, *Appl. Surf. Sci.*, 1996, **107**, 128–136.

116 M. Q. Snyder, S. A. Trebukhova, B. Ravdel, M. C. Wheeler, J. DiCarlo, C. P. Tripp and W. J. DeSisto, Synthesis and characterization of atomic layer deposited titanium nitride thin films on lithium titanate spinel powder as a lithium-ion battery anode, *J. Power Sources*, 2007, **165**(1), 379–385.

117 Y. S. Jung, A. S. Cavanagh, A. C. Dillon, M. D. Groner, S. M. George and S. H. Lee, Enhanced stability of $LiCoO_2$ cathodes in lithium-ion batteries using surface modification by atomic layer deposition, *J. Electrochem. Soc.*, 2010, **157**(1), A75–A81.

118 Y. S. Jung, A. S. Cavanagh, L. A. Riley, S. H. Kang, A. C. Dillon, M. D. Groner, S. M. George and S. H. Lee, Ultrathin direct atomic layer deposition on composite electrodes for highly durable and safe Li-ion batteries, *Adv. Mater.*, 2010, **22**(19), 2172–2176.

119 X. Li, J. Liu, X. Meng, Y. Tang, M. N. Banis, J. Yang, Y. Hu, R. Li, M. Cai and X. Sun, Significant impact on cathode performance of lithium-ion batteries by precisely controlled metal oxide nanocoatings via atomic layer deposition, *J. Power Sources*, 2014, **247**, 57–69.

120 X. Meng, Inhibiting sulfur shuttle behaviors in high-energy lithium-sulfur batteries, *US Patent Application No*. 62/471161, 2017.

121 H. Gao, J. Cai, G.-L. Xu, L. Li, Y. Ren, X. Meng, K. Amine and Z. Chen, Surface modification for suppressing interfacial parasitic reactions of a nickel-rich lithium-ion cathode, *Chem. Mater.*, 2019, **31**(8), 2723–2730.

122 J. Xie, A. D. Sendek, E. D. Cubuk, X. Zhang, Z. Lu, Y. Gong, T. Wu, F. Shi, W. Liu, E. J. Reed and Y. Cui, Atomic layer deposition of stable $LiAlF_4$ lithium ion conductive interfacial layer for stable cathode cycling, *ACS Nano*, 2017, **11**, 7019–7027.

123 A. Shapira, O. Tiurin, N. Solomatin, M. Auinat, A. Meitav and Y. Ein-Eli, Robust AlF3 Atomic Layer Deposition Protective Coating on LiMn1.5Ni0.5O4 Particles: An Advanced Li-Ion Battery Cathode Material Powder, *ACS Appl. Energy Mater.*, 2018, **1**(12), 6809–6823.

124 Y. Cao, X. Meng and J. W. Elam, Atomic layer deposition of Li_xAl_yS solid-state electrolytes for stabilizing lithium-metal anodes, *ChemElectroChem*, 2016, **3**, 858–863.

125 B. Xiao, B. Wang, J. Liu, K. Kaliyappan, Q. Sun, Y. Liu, G. Dadheech, M. P. Balogh, L. Yang, T.-K. Sham, R. Li, M. Cai and X. Sun, Highly stable Li1.2Mn0.54Co0.13Ni0.13O2 enabled by novel atomic layer deposited AlPO4 coating, *Nano Energy*, 2017, **34**, 120–130.

126 C.-F. Lin, X. Fan, A. Pearse, S.-C. Liou, K. Gregorczyk, M. Leskes, C. Wang, S. B. Lee, G. W. Rubloff and M. Noked, Highly Reversible Conversion-Type FeOF Composite Electrode with Extended Lithium Insertion by Atomic Layer Deposition LiPON Protection, *Chem. Mater.*, 2017, **29**(20), 8780–8791.

127 H. Kim, J. T. Lee, D. C. Lee, A. Magasinski, W. I. Cho and G. Yushin, Plasma-Enhanced Atomic Layer Deposition of Ultrathin Oxide Coatings for Stabilized Lithium-Sulfur Batteries, *Adv. Energy Mater.*, 2013, **3**(10), 1308–1315.

128 X. Meng, D. J. Comstock, T. T. Fister and J. W. Elam, Vapor-phase atomic-controllable growth of amorphous Li_2S for high-performance lithium–sulfur batteries, *ACS Nano*, 2014, **8**(10), 10963–10972.

129 J. Lu, Y. Lei, K. C. Lau, X. Luo, P. Du, J. Wen, R. S. Assary, U. Das, D. J. Miller, J. W. Elam, H. M. Albishri, D. A. El-Hady, Y.-K. Sun, L. A. Curtiss and K. Amine, A nanostructured cathode architecture for low charge overpotential in lithium-oxygen batteries, *Nat. Commun.*, 2013, **4**, 2383.

130 L. Zhao, J. Zhao, Y.-S. Hu, H. Li, Z. Zhou, M. Armand and L. Chen, Disodium Terephthalate (Na2C8H4O4) as High

Performance Anode Material for Low-Cost Room-Temperature Sodium-Ion Battery, *Adv. Energy Mater.*, 2012, **2**(8), 962–965.

131 N. D. Schuppert, S. Mukherjee, A. M. Bates, E.-J. Son, M. J. Choi and S. Park, *Ex situ* X-ray diffraction analysis of electrode strain at TiO2 atomic layer deposition/α-MoO3 interface in a novel aqueous potassium ion battery, *J. Power Sources*, 2016, **316**, 160–169.

132 K. Zhao, C. Wang, Y. Yu, M. Yan, Q. Wei, P. He, Y. Dong, Z. Zhang, X. Wang and L. Mai, Ultrathin Surface Coating Enables Stabilized Zinc Metal Anode, *Adv. Mater. Interfaces*, 2018, **5**(16), 1800848.

133 D. Pal, A. Mathur, A. Singh, S. Pakhira, R. Singh and S. Chattopadhyay, Binder-Free ZnO Cathode synthesized via ALD by Direct Growth of Hierarchical ZnO Nanostructure on Current Collector for High-Performance Rechargeable Aluminium-Ion Batteries, *ChemistrySelect*, 2018, **3**(44), 12512–12523.

134 Y. Zhao, L. V. Goncharova, Q. Sun, X. Li, A. Lushington, B. Wang, R. Li, F. Dai, M. Cai and X. Sun, Robust metallic lithium anode protection by the molecular-layer-deposition technique, *Small Methods*, 2018, **2**(5), 1700417.

135 Y. Zhao, L. V. Goncharova, Q. Zhang, P. Kaghazchi, Q. Sun, A. Lushington, B. Wang, R. Li and X. Sun, Inorganic–Organic Coating via Molecular Layer Deposition Enables Long Life Sodium Metal Anode, *Nano Lett.*, 2017, **17**(9), 5653–5659.

136 K. Kaliyappan, T. Or, Y.-P. Deng, Y. Hu, Z. Bai and Z. Chen, Constructing Safe and Durable High-Voltage P2 Layered Cathodes for Sodium Ion Batteries Enabled by Molecular Layer Deposition of Alucone, *Adv. Funct. Mater.*, 2020, **30**(17), 1910251.

137 X. Meng, K. C. Lau, H. Zhou, S. K. Ghosh, M. Benamara and M. Zou, Molecular Layer Deposition of Crosslinked Polymeric Lithicone for Superior Lithium Metal Anodes, *Energy Mater. Adv.*, 2021, **2021**, 9786201.

138 X. Wang, J. Cai, K. Velasquez Carballo, F. Watanabe and X. Meng, Tackling issues of lithium metal anodes with a novel polymeric lithicone coating, *Chem. Eng. J.*, 2023, **475**, 146156.

139 A. C. Kozen, C.-F. Lin, A. J. Pearse, M. A. Schroeder, X. Han, L. Hu, S.-B. Lee, G. W. Rubloff and M. Noked, Next-generation lithium metal anode engineering via atomic layer deposition, *ACS Nano*, 2015, **9**(6), 5884–5892.

140 E. Kazyak, K. N. Wood and N. P. Dasgupta, Improved cycle life and stability of lithium metal anodes through ultrathin atomic layer deposition surface treatments, *Chem. Mater.*, 2015, **27**(18), 6457–6462.

141 P. K. Alaboina, S. Rodrigues, M. Rottmayer and S.-J. Cho, In Situ Dendrite Suppression Study of Nanolayer Encapsulated Li Metal Enabled by Zirconia Atomic Layer Deposition, *ACS Appl. Mater. Interfaces*, 2018, **10**(38), 32801–32808.

142 M. Wang, X. Cheng, T. Cao, J. Niu, R. Wu, X. Liu and Y. Zhang, Constructing ultrathin TiO2 protection layers via atomic layer deposition for stable lithium metal anode cycling, *J. Alloys Compd.*, 2021, **865**, 158748.

143 L. Chen, K.-S. Chen, X. Chen, G. Ramirez, Z. Huang, N. R. Geise, H.-G. Steinrück, B. L. Fisher, R. Shahbazian-Yassar, M. F. Toney, M. C. Hersam and J. W. Elam, Novel ALD Chemistry Enabled Low-Temperature Synthesis of Lithium Fluoride Coatings for Durable Lithium Anodes, *ACS Appl. Mater. Interfaces*, 2018, **10**(32), 26972–26981.

144 J. Niu, M. Wang, T. Cao, X. Cheng, R. Wu, H. Liu, Y. Zhang and X. Liu, Li metal coated with Li3PO4 film via atomic layer deposition as battery anode, *Ionics*, 2021, **27**(6), 2445–2454.

145 W. D. Richards, L. J. Miara, Y. Wang, J. C. Kim and G. Ceder, Interface stability in solid-state batteries, *Chem. Mater.*, 2016, **28**(1), 266–273.

146 L. S. Combes, S. S. Ballard and K. A. McCarthy, Mechanical and Thermal Properties of Certain Optical Crystalline Materials, *J. Opt. Soc. Am.*, 1951, **41**(4), 215–222.

147 S. Yu, R. D. Schmidt, R. Garcia-Mendez, E. Herbert, N. J. Dudney, J. B. Wolfenstine, J. Sakamoto and D. J. Siegel, Elastic Properties of the Solid Electrolyte Li7La3Zr2O12 (LLZO), *Chem. Mater.*, 2016, **28**(1), 197–206.

148 C. Monroe and J. Newman, The Impact of Elastic Deformation on Deposition Kinetics at Lithium/Polymer Interfaces, *J. Electrochem. Soc.*, 2005, **152**(2), A396–A404.

149 J. Xie, L. Liao, Y. Gong, Y. Li, F. Shi, A. Pei, J. Sun, R. Zhang, B. Kong, R. Subbaraman, J. Christensen and Y. Cui, Stitching h-BN by atomic layer deposition of LiF as a stable interface for lithium metal anode, *Sci. Adv.*, 2017, **3**(11), eaao3170.

150 X. Meng, Y. Cao, J. A. Libera and J. W. Elam, Atomic layer deposition of aluminum sulfide: Growth mechanism and electrochemical evaluation in lithium-ion batteries, *Chem. Mater.*, 2017, **29**(21), 9043–9052.

151 X. Meng and J. W. Elam, Atomic-scale rational designs of superionic sulfide-based solid-state electrolytes by atomic layer deposition, *ECS Meet. Abstr.*, 2019, **MA2019-01**(2), 155.

152 L. Chen, Z. Huang, R. Shahbazian-Yassar, J. A. Libera, K. C. Klavetter, K. R. Zavadil and J. W. Elam, Directly formed alucone on lithium metal for high-performance Li batteries and Li-S batteries with high sulfur mass loading, *ACS Appl. Mater. Interfaces*, 2018, **10**(8), 7043–7051.

153 K. R. Adair, C. Zhao, M. N. Banis, Y. Zhao, R. Li, M. Cai and X. Sun, Highly Stable Lithium Metal Anode Interface via Molecular Layer Deposition Zircone Coatings for Long Life Next-Generation Battery Systems, *Angew. Chem., Int. Ed.*, 2019, **58**(44), 15797–15802.

154 Y. Sun, Y. Zhao, J. Wang, J. Liang, C. Wang, Q. Sun, X. Lin, K. R. Adair, J. Luo, D. Wang, R. Li, M. Cai, T.-K. Sham and X. Sun, A novel organic "polyurea" thin film for ultralong-life lithium-metal anodes via molecular-layer deposition, *Adv. Mater.*, 2019, **31**(4), 1806541.

155 X. Wang, J. Cai, Y. Ren, M. Benamara, X. Zhou, Y. Li, Z. Chen, H. Zhou, X. Xiao, Y. Liu and X. Meng, High-performance $LiNi_{0.8}Mn_{0.1}Co_{0.1}O_2$ cathode by nanoscale lithium sulfide coating via atomic layer deposition, *J. Energy Chem.*, 2022, **69**, 531–540.

156 Y. Zhao, M. Amirmaleki, Q. Sun, C. Zhao, A. Codirenzi, L. V. Goncharova, C. Wang, K. Adair, X. Li, X. Yang, F. Zhao, R. Li, T. Filleter, M. Cai and X. Sun, Natural SEI-inspired dual-protective layers via atomic/molecular layer deposition for long-life metallic lithium anode, *Matter*, 2019, **1**(5), 1215–1231.

157 L. Tan, X. Li, T. Liu and X. Li, Atomic layer deposition-strengthened lithiophilicity of ultrathin TiO2 film decorated Cu foil for stable lithium metal anode, *J. Power Sources*, 2020, **463**, 228157.

158 S. T. Oyakhire, W. Huang, H. Wang, D. T. Boyle, J. R. Schneider, C. de Paula, Y. Wu, Y. Cui and S. F. Bent, Revealing and Elucidating ALD-Derived Control of Lithium Plating Microstructure, *Adv. Energy Mater.*, 2020, **10**(44), 2002736.

159 Y. Liu, D. Lin, Z. Liang, J. Zhao, K. Yan and Y. Cui, Lithium-coated polymeric matrix as a minimum volume-change and dendrite-free lithium metal anode, *Nat. Commun.*, 2016, **7**, 10992.

160 K.-H. Chen, A. J. Sanchez, E. Kazyak, A. L. Davis and N. P. Dasgupta, Synergistic Effect of 3D Current Collectors and ALD Surface Modification for High Coulombic Efficiency Lithium Metal Anodes, *Adv. Energy Mater.*, 2019, **9**(4), 1802534.

161 Y. Jiang, Z. Wang, C. Xu, W. Li, Y. Li, S. Huang, Z. Chen, B. Zhao, X. Sun, D. P. Wilkinson and J. Zhang, Atomic layer deposition for improved lithiophilicity and solid electrolyte interface stability during lithium plating, *Energy Storage Mater.*, 2020, **28**, 17–26.

162 B. Zhao, B. Li, Z. Wang, C. Xu, X. Liu, J. Yi, Y. Jiang, W. Li, Y. Li and J. Zhang, Uniform Li Deposition Sites Provided by Atomic Layer Deposition for the Dendrite-free Lithium Metal Anode, *ACS Appl. Mater. Interfaces*, 2020, **12**(17), 19530–19538.

163 R. Zhang, Y. Li, L. Qiao, D. Li, J. Deng, J. Zhou, L. Xie, Y. Hou, T. Wang, W. Tian, J. Cao, F. Cheng, B. Yang, K. Liang, P. Chen and B. Kong, Atomic layer deposition assisted superassembly of ultrathin ZnO layer decorated hierarchical Cu foam for stable lithium metal anode, *Energy Storage Mater.*, 2021, **37**, 123–134.

164 Y. Zhang, B. Liu, E. Hitz, W. Luo, Y. Yao, Y. Li, J. Dai, C. Chen, Y. Wang, C. Yang, H. Li and L. Hu, A carbon-based 3D current collector with surface protection for Li metal anode, *Nano Res.*, 2017, **10**(4), 1356–1365.

165 R. Tian, X. Feng, H. Duan, P. Zhang, H. Li, H. Liu and L. Gao, Low-Weight 3D Al_2O_3 Network as an Artificial Layer to Stabilize Lithium Deposition, *ChemSusChem*, 2018, **11**(18), 3243–3252.